

Group-blind optimal transport to group parity and its constrained variants

Quan Zhou

*Dyson School of Design Engineering
Imperial College London
London SW72AZ, UK*

Q.ZHOU22@IMPERIAL.AC.UK

Jakub Mareček

*Department of Computer Science
Czech Technical University in Prague
Prague 12135, the Czech Republic*

JAKUB.MARECEK@FEL.CVUT.CZ

Abstract

Fairness holds a pivotal role in the realm of machine learning, particularly when it comes to addressing groups categorised by sensitive attributes, e.g., gender, race. Prevailing algorithms in fair learning predominantly hinge on accessibility or estimations of these sensitive attributes, at least in the training process. We design a single group-blind projection map that aligns the feature distributions of both groups in the source data, achieving (demographic) group parity, without requiring values of the protected attribute for individual samples in the computation of the map, as well as its use. Instead, our approach utilises the feature distributions of the privileged and unprivileged groups in a boarder population and the essential assumption that the source data are unbiased representation of the population. We present numerical results on synthetic data and real data.

1 Introduction

Fairness is a crucial consideration in machine learning to avoid biased and discriminatory results, protect individuals and groups, build trust, comply with legal and ethical requirements, and ultimately improve the impact of machine learning systems (Mehrabi et al., 2021; Osoba and Welser IV, 2017). In many applications, where machine learning underlies business practices, societal interactions, and policy-making, fairness is crucial to ensure that environmental, social and governance criteria are met (Friede et al., 2015, ESG), which in turn promote sustainable business practises and foster positive societal impact.

It is well understood (Angwin et al., 2022; Mhasawade et al., 2021; Calders and Žliobaitė, 2013) that seemingly neutral machine learning models and algorithms are capable of disproportionately negative effects on certain individuals or groups based on their membership in a protected class or demographic category, even if no sensitive attribute is used, their use in other settings can be judged fair, and there is no explicit intention to discriminate. This is particularly important in the context of so-called foundational models, which are trained on a large dataset without focusing on a single application and then adapted to a new domain using transfer learning.

To mitigate the disparate impact in classification, two common strategies have been employed in transfer learning and beyond. The first strategy directly adjusts the values of features, labels, model outputs (estimated labels) or any combination thereof. Initially,

Zemel et al. (2013) proposed a mapping to some fair representations of features. Feldman et al. (2015) suggested modifying features so that the distributions for privileged and unprivileged groups become similar to a “median” distribution, making it harder for the algorithm to differentiate between the two groups. The principle has been expanded to adjusting both features and the label in Calmon et al. (2017) and further to projecting distributions of features to a barycenter (Gordaliza et al., 2019; Yang et al., 2022), which introduces the least data distortion. Oneto and Chiappa (2020); Chzhen et al. (2020); Gouic et al. (2020) performed post-processing of the model outputs by transporting the distributions of the outputs of each group to a barycenter. Jiang and Nachum (2020) corrected for a range of biases by reweighting the training data.

The second strategy incorporates a regularisation term to penalise discriminatory effects whilst building some classification or prediction models. Quadrianto and Sharmanska (2017) designed regularisation components using the maximum mean discrepancy criterion of Gretton et al. (2012) to encourage the similarity of the distributions of the prediction outputs across the privileged and unprivileged groups, with the assumption of sensitive attributes only available at training time. Jiang et al. (2020) used Wasserstein distance of the distributions of outputs between privileged and unprivileged groups as the regularisation in logistic regression, again without any requirements on the availability of the sensitive attribute at test time. The Wasserstein regularisation is also used in neural-network classifiers (Risser et al., 2022) and various applications (Jourdan et al., 2023) thereof. Buyl and De Bie (2022) design a regularisation term by the minimum cost to transport a classifier’s score function to a set of fair score functions, and generalise the fairness measures allowed.

A key challenge, which has not been explored in depth, is the availability of protected attributes (e.g., gender, race). In practise, protected attributes are generally unavailable or inaccessible. In many jurisdictions, businesses cannot collect data on the race of their customers, for example, for any purpose whatsoever. In the European Union, the proposed AI act will make it possible to collect protected attributes in so-called sandboxes to audit the fairness of algorithms, but not to train the algorithms. In contrast, most fairness-aware algorithms and techniques that incorporate group fairness are based on the assumption that sensitive attributes are accessible. All the methods mentioned above use the sensitive attribute of each sample (data point) as a prerequisite for modifying the values differently for different groups (in the first strategy), or measuring the loss of group-fairness regularisation term in iterations of training the classification or prediction models (in the second strategy).

The challenge of the availability of protected attributes has been partially addressed by Oneto and Chiappa (2020); Jiang et al. (2020); Quadrianto and Sharmanska (2017); Zafar et al. (2017a), who considered sensitive attributes at training time, and by Chai and Wang (2022), who leverages a small validation set with sensitive attributes to help guide training. Wang et al. (2020); Amini et al. (2019); Oneto et al. (2019) relaxed the strict requirement of the sensitive attribute being available, and use some noisy estimate instead. Sohoni et al. (2020) considered clustering to a similar effect. Finally, Liu et al. (2023); Andrus and Villeneuve (2022) aimed to mitigate bias and ensure fairness without relying on explicit group definitions.

Contributions We introduce novel methods for removing disparate impact in transfer learning (also known as domain adaptation and fairness repair), without requiring the pro-

tected attribute to be revealed. Our methods are related to the “total repair” and “partial repair” schemes of Feldman et al. (2015) and Gordaliza et al. (2019), which project the distributions of features for privileged and unprivileged groups to a target distribution interpolating between the groups. However, the previous schemes (Gordaliza et al., 2019; Feldman et al., 2015) require the sensitive attribute to define groups, while the sensitive attribute is either simply unavailable, or even illegal to collect in many settings.

Our work follows the idea (Quinn et al., 2023, Slide 23) to use marginals from another data set in transfer learning towards a data set whose bias is, at least in part, determined by an unavailable protected attribute. In the setting envisioned by the AI Act in the European Union, this additional data set could be collected within so-called regulatory sandbox Allen (2019); Morgan (2023), wherein a regulator and the developer of an AI system agree to override data privacy protection in a well-defined fashion. In many other settings, the data could be collected in the census. When no such data exists, such as when France bars the collection of data on the race and ethnicity of its citizens even in the census (Ndiaye, June 13th, 2020), or India bars the collection of data on caste status in its census (Bose et al., October 12th, 2023), it would seem difficult to address the bias, indeed.

We develop algorithms to realise this objective. The membership of each sample is used to calculate distinct projections for various groups and to modify the value of features via group-wise projections. We extend these schemes to modifying the values of features via one group-blind projection map, and achieve equalised distributions of modified features between privileged and unprivileged groups. The sample membership is not required for computing such group-blind projection map, or for modifying the values of features via this group-blind projection map. We require only the population-level information regarding feature distributions for both privileged and unprivileged groups, as well as the assumptions that source data are collected via unbiased sampling from the population. The target distribution in our framework is not necessarily the barycentre distribution. Instead, since the modified or projected data will be used on a pre-trained classification or prediction model, the distribution of training data used to learn such a pre-trained model can be our target distribution, to preserve the classification or prediction performance.

Paper structure The paper is organised as follows: Section 1.1 gives the motivating example of school admission. Section 1.2 introduces related work. Section 2 presents the state-of-the-art in entropic regularised OT. Section 3 introduces our “total repair” and “partial repair” schemes with our algorithm. Sections 3.1-3.4 focus on a one-dimensional case (that is, only one unprotected feature is considered) and Section 3.5 explains how to implement our schemes in higher-dimensional cases. Section 3.6 explains the choices of target distribution. Section 4 gives the numerical results on synthetic data and real-world data, as well as a comparison with two baselines. The proofs of all lemmas and theorems can be found in Appendices.

1.1 Motivating example

Let us consider an example of school admission to illustrate the bias repair schemes in our framework as well as Gordaliza et al. (2019); Feldman et al. (2015). Schools commonly use exam scores to make admission decisions with a cutoff point: students with scores higher than the cutoff point will be admitted. In Figure 1, this is shown with the vertical

dashed line. The applicants can be divided into two groups by a sensitive attribute, e.g., gender, race. The left subplot of Figure 1 shows that the score distribution of the privileged group (denoted by a purple curve) concentrates somewhere above the cut-off point. On the contrary, only a small portion of the unprivileged group (denoted by an orange curve) passes the cut-off point. If the cutoff point is used in a straightforward manner, the admission results are strongly biased against the unprivileged group, although the admission-decision algorithm does not take into account the sensitive attribute. Then, instead of training another fairness-aware admission-decision model, the bias repair schemes will project the score distributions of both groups into an arbitrary target distribution, for example, the green curve, such that the scores of both groups follow the same target distribution. The target distribution is a “median” distribution in Feldman et al. (2015), and a barycentre distribution in Gordaliza et al. (2019), and are not necessarily the same as the green curve.

The right subplots of Figure 1 illustrate the effects of bias-repair schemes proposed in this paper, with the top two for “partial repair”, and the bottom one for “total repair”. Now, the same admission cut-off point used on the projected scores will achieve equalised admission rates between the privileged and the unprivileged group. Our extension eliminates the need for the sensitive attribute of each sample when computing the group-blind projection map and projecting both groups via this map.

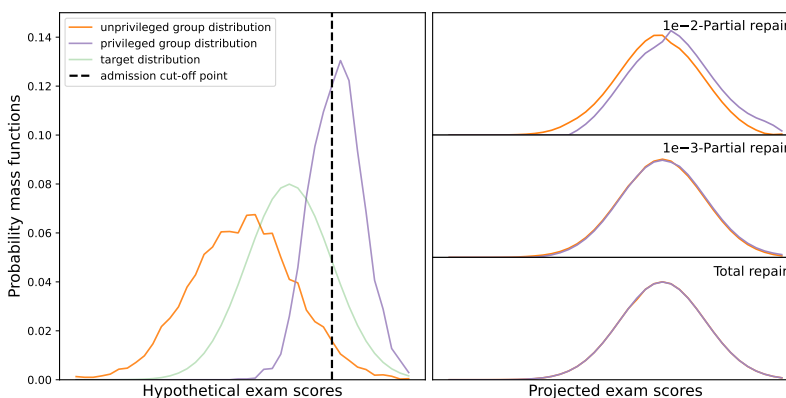


Figure 1: **Left:** A cut-off point (vertical dark line) for an exam score is used to make school-admission decisions. With the hypothetical exam-score distributions of the unprivileged group (orange) and the privileged group (purple), this group-blind cut-off point would result in outcomes biased against the unprivileged group. If the score distributions of unprivileged group and the privileged group are projected closer to an arbitrary target distribution (green), the same cut-off point can achieve equalised admission rates. **Right:** The partial repair (top two) and total repair (bottom) schemes proposed in this paper, move the score distributions of unprivileged group (orange) and the privileged group (purple) closer to the pre-defined target distribution, without access to the sensitive attribute of each sample in training process.

1.2 Related work

Fairness in machine learning There are various definitions and metrics of fairness, nicely surveyed in Castelnovo et al. (2022); Pessach and Shmueli (2022); Mehrabi et al. (2021). Different fairness criteria may conflict with each other Kim et al. (2020); Binns (2020). The category of group fairness stands out as the most extensively studied, comprising demographic parity addressing disparate impact, fairness through unawareness (Fabris et al., 2023) addressing disparate treatment, equal opportunity (Hardt et al., 2016) and predictive equality (Zeng et al., 2022; Chouldechova, 2017), both of which address disparate mistreatment (Zafar et al., 2019, 2017b). Fairness measures have been extended to individual fairness (Petersen et al., 2021; Dwork et al., 2012), procedural fairness (Grgić-Hlača et al., 2018), as well as (path-specific) counterfactual fairness (Kusner et al., 2017; Chiappa, 2019; Nabi et al., 2022; Plecko and Bareinboim, 2022; Nilforoshan et al., 2022).

Multiple studies have extensively examined the trade-offs that arise between fairness and accuracy in Liu and Vicente (2022); Mandal et al. (2020), the trade-offs between group fairness and individual fairness in Binns (2020), and the trade-offs between fairness and privacy in Chang and Shokri (2021); Cummings et al. (2019). There have been designs of systems to balance multiple potentially conflicting fairness measures Kim et al. (2020); Lohia et al. (2019). These fairness criteria have been used in fair classification (Zafar et al., 2019; Barocas et al., 2019), fair prediction (Plecko and Bareinboim, 2022; Chouldechova, 2017), fair ranking (Narasimhan et al., 2020; Feldman et al., 2015), fair policy (Plecko and Bareinboim, 2023; Chzhen et al., 2021; Nabi et al., 2019), and fair representation in (Zhao and Gordon, 2022; Creager et al., 2019; Zemel et al., 2013). In the long term, maintaining machine learning models adaptable to dynamic fairness concepts, due to evolving data distributions, or changing societal norms, has been considered (Bechavod and Roth, 2023; Jabbari et al., 2017).

Optimal transport We refer to Peyré et al. (2019) for a comprehensive overview of the history of optimal transport (OT). It is a method to find a coupling that moves mass from one distribution to another at the smallest possible cost, known as the Monge problem, relaxed into so-called Kantorovich relaxation. The relaxation, with an entropic regularisation to promote smoothness of the map, leads to iterations of simple matrix-vector products of the Sinkhorn–Knopp algorithm (Sinkhorn and Knopp, 1967). Often, the equality constraints in entropy-regularised OT are softened by minimising the dual norm of the differences between both sides of equality constraints; see Chapel et al. (2021); Pham et al. (2020); Chizat et al. (2018a) for unbalanced OT and Chizat et al. (2018b) for dynamic unbalanced OT. Pioneered by Gangbo and Świech (1998); Agueh and Carlier (2011), another direction is to explore barycentres of Wasserstein distance of multiple distributions with respect to some weights, which is a representation of the mean of the set of distributions, with several follow-up works in Nath and Jawanpuria (2020); Dard et al. (2016); Seguy and Cuturi (2015). On the computational side, the simplest algorithm that exploits Kullback-Leibler (KL) divergence is the iterative Bregman projections (Bregman, 1967), which is related to the Sinkhorn algorithm. The generic OT considering finitely many arbitrary convex constraints can be solved by Dykstra’s algorithm with Bregman projections (Bauschke and Lewis, 2000; Benamou et al., 2015), or generalised scaling algorithm (Chizat et al., 2018a). The mini-batch OT can be used to ease the computational burden (Sommerfeld

et al., 2019). The classic OT formulation with entropic regularisation penalty, together with its generalisations is explained in Section 2.1.

OT has been widely used in domain adaptation (Turrisi et al., 2022; Nguyen et al., 2022; Courty et al., 2017) by computing a map that project the distributions of multiple datasets into a common representation. See Montesuma et al. (2023) for a survey. The same principle of using OT as a projection map could be used to mitigate algorithmic bias in machine-learning models (Gordaliza et al., 2019; Silvia et al., 2020; Yang et al., 2022). Utilisation of OT as a loss or a metric has emerged as a notable trending subject within bias mitigation (Buyl and De Bie, 2022; Risser et al., 2022; Jiang et al., 2020; Oneto and Chiappa, 2020) and bias detection (Si et al., 2021; Black et al., 2020).

2 Background and Notation

Let N be the number of discretisation points, and $P \in \mathbb{R}^N$ be vectors in the probability simplex:

$$\Sigma_N := \left\{ P \in \mathbb{R}_+^N \mid \sum_{i=1}^N P_i = 1 \right\}. \quad (1)$$

The set of all admissible or feasible couplings between $(P, Q) \in \Sigma_N^2$ is defined as

$$\Pi(P, Q) := \{ \gamma \in \mathbb{R}_+^{N \times N} \mid \gamma \mathbf{1} = P, \gamma^{\text{tr}} \mathbf{1} = Q \}, \quad (2)$$

where $\mathbf{1}$ is the N -dimensional column vector of ones, γ^{tr} is the transpose of γ . Further, we define the entropy of a coupling γ as:

$$E(\gamma) := - \sum_{i,j=1}^N \gamma_{i,j} (\log(\gamma_{i,j}) - 1), \quad (3)$$

which is concave function and we use the convention $0 \log 0 = 0$. The Kullback-Leibler (KL) divergence between the coupling $\gamma \in \mathbb{R}_+^{N \times N}$ and a positive reference matrix $\xi \in \mathbb{R}_{++}^{N \times N}$ (i.e., $\xi_{i,j} > 0$) is defined as:

$$\text{KL}(\gamma \parallel \xi) := \sum_{i,j=1}^N \gamma_{i,j} \left(\log \left(\frac{\gamma_{i,j}}{\xi_{i,j}} \right) - 1 \right). \quad (4)$$

Given a convex set $\mathcal{C} \in \mathbb{R}^{N \times N}$, the KL projection is

$$\mathcal{P}_{\mathcal{C}}^{\text{KL}}(\xi) := \arg \min_{\gamma \in \mathcal{C}} \text{KL}(\gamma \parallel \xi), \quad (5)$$

which is uniquely defined since KL divergence is a strictly convex and coercive function and, \mathcal{C} is a convex set. See Lemma 13 for more details.

2.1 Regularised Optimal Transport

Referring to Benamou et al. (2015), we introduce the state of the art in OT. The discrete entropic regularisation OT problem has the form:

$$W_{\epsilon}(P, Q) := \min_{\gamma \in \Pi(P, Q)} \langle C, \gamma \rangle - \epsilon E(\gamma), \quad (6)$$

where $C \in \mathbb{R}^{N \times N}$ is the cost matrix, $\epsilon > 0$ is the entropic regularisation parameter and $\langle \cdot, \cdot \rangle$ is the inner product. This formulation is equivalent to

$$\begin{aligned} W_\epsilon(P, Q) &= \min_{\gamma \in \Pi(P, Q)} \sum_{i,j=1}^N C_{i,j} \gamma_{i,j} + \epsilon \gamma_{i,j} (\log(\gamma_{i,j}) - 1) \\ &= \min_{\gamma \in \Pi(P, Q)} \epsilon \sum_{i,j=1}^N \gamma_{i,j} (\log(\gamma_{i,j}) - \log(\exp(-C_{i,j}/\epsilon)) - 1) \\ &= \min_{\gamma \in \Pi(P, Q)} \epsilon \text{KL}(\gamma \| \xi), \quad \text{where } \xi = \exp(-C/\epsilon). \end{aligned} \tag{7}$$

Further, the set of admissible (feasible) couplings in Equation (2) could be formulated as the intersection of two affine subspaces: $\Pi(P, Q) = \mathcal{C}_1 \cap \mathcal{C}_2$, where

$$\mathcal{C}_1 := \{\gamma \in \mathbb{R}_+^{N \times N} \mid \gamma \mathbf{1} = P\}, \quad \mathcal{C}_2 := \{\gamma \in \mathbb{R}_+^{N \times N} \mid \gamma^{\text{tr}} \mathbf{1} = Q\}. \tag{8}$$

Generally, when the convex sets $\mathcal{C}_\ell, \ell \geq 1$ are affine subspaces, initialise $\gamma^{(0)} := \xi = \exp(-C/\epsilon)$, then conduct iterative KL projections: for $n > 0$

$$\gamma^{(n+1)} = \mathcal{P}_{\mathcal{C}_n}^{\text{KL}}(\gamma^{(n)}), \tag{9}$$

where $\mathcal{C}_n \equiv \mathcal{C}_{1+(n \bmod 2)}$. The iterations in Equation (9) can converge to the unique solution of $W_\epsilon(P, Q)$, as $n \rightarrow +\infty$ (Fact 1.4 in Bauschke et al. (2020), Benamou et al. (2015); Bregman (1967)). Note that the KL projections used in the paper, is a special case of the general Bregman projections as in Definition 22.

Inequality constraints When the convex sets are not affine subspaces, iterative Bregman projections do not converge to $W_\epsilon(P, Q)$ (Fact 1.2 in Bauschke et al. (2020)). Instead, Dykstra’s algorithm is known to converge when used in conjunction with Bregman divergences, for arbitrary convex sets (cf. Appendix J or Bauschke et al. (2020); Bauschke and Lewis (2000)). Random Dykstra algorithm converges linearly in expectation for the general feasible sets satisfying Slater’s condition (Necoara and Fercoq, 2022).

It could be used to solve OT problem with inequality constraints:

Example 1 *The partial OT (Le et al., 2022; Caffarelli and McCann, 2010; Figalli, 2010) only needs to transport a given fraction of mass and the two marginals P, Q do not need to have the same total mass:*

$$\min_{\gamma \in \mathbb{R}_+^{N \times N}} \{\langle C, \gamma \rangle - \epsilon E(\gamma) \mid \gamma \mathbf{1} \leq P, \gamma^{\text{tr}} \mathbf{1} \leq Q, \mathbf{1}^{\text{tr}} \gamma \mathbf{1} = \eta\},$$

where the constant $\eta \in [0, \min\{P^{\text{tr}} \mathbf{1}, Q^{\text{tr}} \mathbf{1}\}]$ denotes the fraction of mass needed to transport. Similarly, this problem can be reformulated as Equation (7) but with γ falling into the intersection of three convex sets:

$$\mathcal{C}_1 := \{\gamma \in \mathbb{R}_+^{N \times N} \mid \gamma \mathbf{1} \leq P\}, \quad \mathcal{C}_2 := \{\gamma \in \mathbb{R}_+^{N \times N} \mid \gamma^{\text{tr}} \mathbf{1} \leq Q\}, \quad \mathcal{C}_3 := \{\gamma \in \mathbb{R}_+^{N \times N} \mid \mathbf{1}^{\text{tr}} \gamma \mathbf{1} = \eta\}.$$

Example 2 *The capacity constrained OT, pioneered by Korman and McCann (2015, 2013), is imposed by an extra upper bound on the amount of mass transported from i to j . Its formulation reads:*

$$\min_{\gamma \in \mathbb{R}_+^{N \times N}} \{ \langle C, \gamma \rangle - \epsilon E(\gamma) \mid \gamma \mathbb{1} = P, \gamma^{\text{tr}} \mathbb{1} = Q, \gamma \leq \Theta \},$$

where $\Theta \in \mathbb{R}_+^{N \times N}$ denotes the upper bound. We equivalently write the feasible set into the intersection of the following three convex sets:

$$\mathcal{C}_1 := \{ \gamma \in \mathbb{R}_+^{N \times N} \mid \gamma \mathbb{1} = P \}, \quad \mathcal{C}_2 := \{ \gamma \in \mathbb{R}_+^{N \times N} \mid \gamma^{\text{tr}} \mathbb{1} = Q \}, \quad \mathcal{C}_3 := \{ \gamma \in \mathbb{R}_+^{N \times N} \mid \gamma \leq \Theta \}.$$

Computation of KL projections In general, it is impossible to directly compute the KL projections in closed form, so some form of subiterations are required. Notably, the convex set with the form in Equation (8), Example 1-2 can be computed by some matrix-vector multiplications (Benamou et al., 2015), with the min, division operators being element-wise:

$$\mathcal{P}_{\mathcal{C}}^{KL}(\bar{\gamma}) = \begin{cases} \text{diag} \left(\frac{P}{\bar{\gamma} \mathbb{1}} \right) \bar{\gamma} & \text{if } \mathcal{C} = \{ \gamma \in \mathbb{R}_+^{N \times N} \mid \gamma \mathbb{1} = P \}, \\ \bar{\gamma} \text{diag} \left(\frac{Q}{\bar{\gamma}^{\text{tr}} \mathbb{1}} \right) & \text{if } \mathcal{C} = \{ \gamma \in \mathbb{R}_+^{N \times N} \mid \gamma^{\text{tr}} \mathbb{1} = Q \}, \\ \text{diag} \left(\min \left\{ \mathbb{1}, \frac{P}{\bar{\gamma} \mathbb{1}} \right\} \right) \bar{\gamma} & \text{if } \mathcal{C} = \{ \gamma \in \mathbb{R}_+^{N \times N} \mid \gamma \mathbb{1} \leq P \}, \\ \bar{\gamma} \text{diag} \left(\min \left\{ \mathbb{1}, \frac{Q}{\bar{\gamma}^{\text{tr}} \mathbb{1}} \right\} \right) & \text{if } \mathcal{C} = \{ \gamma \in \mathbb{R}_+^{N \times N} \mid \gamma^{\text{tr}} \mathbb{1} \leq Q \}, \\ \bar{\gamma} \frac{\eta}{\mathbb{1}^{\text{tr}} \bar{\gamma} \mathbb{1}} & \text{if } \mathcal{C} = \{ \gamma \in \mathbb{R}_+^{N \times N} \mid \mathbb{1}^{\text{tr}} \gamma \mathbb{1} = \eta \}, \\ \min \{ \bar{\gamma}, \Theta \} & \text{if } \mathcal{C} = \{ \gamma \in \mathbb{R}_+^{N \times N} \mid \gamma \leq \Theta \}, \end{cases}$$

where the proof for the first two cases can be found in Appendix G.

3 Our Framework

Recall the school admission example introduced in Section 1.1. The school receive the exam score (X), but not the sensitive attribute (S) of each applicant. So, the source data would be all applicants' exam scores. Due to S being not observed, the school wants to find a S -blind projection map (\mathcal{T}), to project these scores to the target data, where the two groups of applicants have the same (“total repair”) or equalised (“partial repair”) distributions of scores. In other words, the school wants to achieve equalised odds of admission between the privileged and unprivileged groups in the target data, using the pre-trained admission-decision policy.

3.1 Definitions

Let us introduce our “total repair” and “partial repair” schemes, starting with defining the sensitive attribute (S), distributions of the exam scores (X) and S -blind projection map (\mathcal{T}):

Definition 1 (A sensitive attribute) *Let $S \in \mathbb{N}$ be an integer random variables of a sensitive attribute (e.g., race, gender). Let $P_s^S := \Pr[S = s]$ be the probability of $S = s$. Its support is defined as*

$$\text{supp}(S) := \{ s \in \mathbb{N} \mid \Pr[S = s] > 0 \}. \quad (10)$$

Definition 2 (Source variables of an unprotected attribute) Let $X, X_s, s \in \text{supp}(S)$ be scalar discrete random variables of an unprotected attribute (e.g., income, credit scores), with their supports $\text{supp}(X_s) \subseteq \text{supp}(X) \subset \mathbb{R}$, for $s \in \text{supp}(S)$. Let $\text{supp}(X)$ be N discretisation points. Their probability distributions are taken from the probability simplex $P^X, P^{X_s} \in \Sigma_N$:

$$P_i^X := \Pr[X = i], \quad P_i^{X_s} := \Pr[X = i \mid S = s], \quad (11)$$

where $\Pr[X = i]$ is the probability of $X = i$ and $\Pr[X = i \mid S = s]$ is the conditional probability of $X = i$ when $S = s$.

To an exploration, throughout the paper we only consider the case of two groups, i.e., $\text{supp}(S) = \{s_0, s_1\}$. we assume X includes one unprotected attribute till Section 3.4 and the extension to multiple unprotected attributes will be discussed in Section 3.5.

Next, we define the target distribution, for instance, the ideal score distribution that we want to achieve in the target data. The choice of target distribution will be mentioned in Section 3.6.

Definition 3 (Target variables of the unprotected attribute) Let $\tilde{X}, \tilde{X}_s, s \in \text{supp}(S)$ be scalar discrete random variables, with their supports $\text{supp}(\tilde{X}_s) \subseteq \text{supp}(\tilde{X}) \subset \mathbb{R}$, for $s \in \text{supp}(S)$. Let $\text{supp}(\tilde{X})$ be N discretisation points. Their probability distributions are taken from the probability simplex $P^{\tilde{X}}, P^{\tilde{X}_s} \in \Sigma_N$:

$$P_j^{\tilde{X}} := \Pr[\tilde{X} = j], \quad P_j^{\tilde{X}_s} := \Pr[\tilde{X} = j \mid S = s], \quad (12)$$

In our setting, we would like to map the source data, i.e., samples from the tuple (X, S) to the target data, i.e., samples from the tuple (\tilde{X}, S) , via a projection map \mathcal{T} , that is defined to be S -blind, and induced by a coupling $\gamma \in \Pi(P^X, P^{\tilde{X}})$:

Definition 4 (Projection) Once the coupling $\gamma \in \Pi(P^X, P^{\tilde{X}})$ has been computed, to find the map that transports source data to target data, we define the projection \mathcal{T} :

$$\mathcal{T} : \text{supp}(X) \rightarrow \text{supp}(\tilde{X}) \times \mathbb{R}_+ \\ i \mapsto (j, w_{i,j}), \forall j \in \text{supp}(\tilde{X}), \quad \text{where } w_{i,j} = \frac{\Pr[X = i, \tilde{X} = j]}{\Pr[X = i]} = \frac{\gamma_{i,j}}{P_i^X}.$$

A sample (i, s) is hence split into a sequence of weighted samples $\{(j, w_{i,j}, s)\}_{j \in \text{supp}(\tilde{X})}$. Very importantly, we stress that the projection do not change s and any other features even though s is not observed.

Example 3 Given a sample (i, s) and $\gamma_{i,j} = P_i^X$. Thus $\gamma_{i,j'} = 0$ for $j' \in \text{supp}(\tilde{X}) \setminus \{j\}$ and

$$\mathcal{T}(i) = (j, 1).$$

Hence, this sample is transported to $(j, 1, s)$.

Example 4 Given a sample (i, s) and $\gamma_{i,j} = \gamma_{i,j'} = P_i^X/2$. Thus $\gamma_{i,j^\dagger} = 0$ for $j^\dagger \in \text{supp}(\tilde{X}) \setminus \{j, j'\}$ and

$$\mathcal{T}(i) = \begin{pmatrix} (j, 1/2) \\ (j', 1/2) \end{pmatrix}.$$

Hence, this sample is split into $(j, 1/2, s)$ and $(j', 1/2, s)$.

Observations So far, we have defined the projection map \mathcal{T} in the formal way. We first observe something interesting:

Let $\text{supp}(S) = \{s_0, s_1\}$, $\text{supp}(X) = \{i, i'\}$, $\text{supp}(\tilde{X}) = \{j, j'\}$. Then, our data only include six samples:

$$\begin{aligned} & (i, s_0), (i, s_1), (i, s_1), \\ & (i', s_0), (i', s_0), (i', s_1). \end{aligned}$$

From the source data, we can directly compute $P^X = [1/2, 1/2]^{tr}$, $P^{X_{s_0}} = [1/3, 2/3]^{tr}$ and $P^{X_{s_1}} = [2/3, 1/3]^{tr}$.

If we set entries $\gamma_{i,j} = \gamma_{i',j'} = 1/2$, and $\gamma_{i,j'} = \gamma_{i',j} = 0$, following Example 3, the projected data become:

$$\begin{aligned} & (j, 1, s_0), (j, 1, s_1), (j, 1, s_1), \\ & (j', 1, s_0), (j', 1, s_0), (j', 1, s_1), \end{aligned}$$

such that $P^{\tilde{X}} = P^X$, $P^{\tilde{X}_{s_0}} = P^{X_{s_0}}$, $P^{\tilde{X}_{s_1}} = P^{X_{s_1}}$. Nothing has changed. However, if we set entries $\gamma_{i,j} = \gamma_{i',j'} = \gamma_{i,j'} = \gamma_{i',j} = 1/4$, following Example 4, the projected data become:

$$\begin{aligned} & (j, 1/2, s_0), (j, 1/2, s_0), (j, 1/2, s_0), (j, 1/2, s_1), (j, 1/2, s_1), (j, 1/2, s_1), \\ & (j', 1/2, s_0), (j', 1/2, s_0), (j', 1/2, s_0), (j', 1/2, s_1), (j', 1/2, s_1), (j', 1/2, s_1), \end{aligned}$$

such that $P^{\tilde{X}} = P^X = P^{\tilde{X}_{s_0}} = P^{\tilde{X}_{s_1}}$. This is a trivial example indeed, but it hints at the possibility of manipulating $P^{\tilde{X}_{s_0}}$ and $P^{\tilde{X}_{s_1}}$ by a well-designed S -blind map.

Next, we explain how to extend the observations to nontrivial cases.

3.2 Total Repair

In the school admission example, even when the sensitive attribute S is not observed, and the map is S -blind, we would like to achieve some parity between groups partitioned by S , in the exam score distributions. Formally,

Definition 5 (Total repair) *Following the definition of total repair in Gordaliza et al. (2019), we say that total repair is satisfied if*

$$P^{\tilde{X}_s} = P^{\tilde{X}_{s'}}, \forall s, s' \in \text{supp}(S). \quad (13)$$

Note that when total repair is satisfied, it holds $P^{\tilde{X}_s} = P^{\tilde{X}_{s'}} = P^{\tilde{X}}$.

Lemma 6 *If the coupling $\gamma \in \Pi(P^X, P^{\tilde{X}})$ is given,*

$$P^{\tilde{X}_s} = \gamma^{\text{tr}} \frac{P^{X_s}}{P^X}, \quad P^{\tilde{X}} = \gamma^{\text{tr}} \mathbf{1}, \quad (14)$$

where the division operator is element-wise.

Proof See Appendix A. ■

Intuitive verification Alternatively, we can think about the source data where the probability equals to the proportion. We select all samples that belong to group s : $\{(i_m, s)\}_{m=1, \dots, M}$. Since the projection does not change s , a sample (j, s) in the target data only originates from sample $(i, s), i \in \text{supp}(X)$ in the source data. Now, we equivalently group the same samples and use the number of the same samples as the weight. For instance, if we have five samples of (i, s) , we only use one weighted sample $(i, w_i = 5, s)$ to represent all of them. Since we assume that probability equals portion, the source data can be rewritten as

$$\{(i, w_i, s)\}_{i \in \text{supp}(X_s)}, \quad (15)$$

where $w_i = M \times \Pr[X = i | S = s]$ for $i \in \text{supp}(X_s)$. From the weighted source data, we can compute $\Pr[X = i | S = s] = w_i/M$. Recall Definition 4: a sample (i, s) , or equivalently a weighted sample $(i, w_i = 1, s)$, is transported to a sequence of weighted samples $\{(j, 1 \times w_{i,j}, s)\}_{j \in \text{supp}(\tilde{X})}$. Then the weighted sample (i, w_i, s) is transported to $(j, w_i \times w_{i,j}, s)$ for $j \in \text{supp}(\tilde{X})$. After projecting all samples in weighted source data (Equation (15)), the projected data become

$$\{(j, w_i \times w_{i,j}, s)\}_{i \in \text{supp}(X_s), j \in \text{supp}(\tilde{X})}.$$

Hence, we can compute

$$\Pr[\tilde{X} = j | S = s] = \sum_{i \in \text{supp}(X_s)} w_{i,j} \times w_i / M = \sum_{i \in \text{supp}(X_s)} \Pr[X = i | S = s] \frac{\Pr[X = i, \tilde{X} = j]}{\Pr[X = i]}.$$

Rewrite the above equation in matrix form, and setting the undefined conditional probability to $\Pr[X = i | S = s] = 0$ for $i \in \text{supp}(X) \setminus \text{supp}(X_s)$, we get the same results as in Lemma 6.

Next, we explore what kind of couplings can guarantee total repair in the target data, such that the total repair property is transformed into a constraint imposed on the coupling:

Theorem 7 (Total repair to a constraint on the coupling γ) *In the case of binary sensitive attributes, i.e., $\text{supp}(S) = \{s_0, s_1\}$, if one wishes to achieve total repair, the coupling should satisfy*

$$P^{\tilde{X}_0} - P^{\tilde{X}_1} = \gamma^{\text{tr}} \left(\frac{P^{X_{s_0}} - P^{X_{s_1}}}{P^X} \right) = \gamma^{\text{tr}} V = \mathbf{0}, \quad (16)$$

where the division and subtraction operations are element-wise, and $\mathbf{0} \in \mathbb{R}^N$ is a zero vector. In particular, the vector $V \in \mathbb{R}^N$, is defined as

$$V := \frac{P^{X_{s_0}} - P^{X_{s_1}}}{P^X}, \quad (17)$$

is the most important input in our framework, which only needs $P^{X_{s_0}}, P^{X_{s_1}}$ and P^X to be computed. Note that P^X is already known due to observability of the feature X in source data. While S is not observed, $P^{X_{s_0}}, P^{X_{s_1}}$ can be obtained from the population-level information regarding the distributions of features for both groups (s_0 and s_1), given the crucial assumption that the source data represents unbiased samples from the broader population. This assumption of unbiased sampling ensures that statistical properties of the population carry over.

Proof See Appendix B. ■

Remark 8 (Properties of the vector V) The vector V , defined in Theorem 7, has the following properties.

(i) $(P^X)^{\text{tr}}V = 0$.

(ii) Entries of the vector V are neither all negative nor all positive.

(iii) For a vector $P \in \mathbb{R}^N$, let the l_1 norm of this vector be $\|P\|_1 := \sum_{i=1}^N |P_i|$. If the norm $\|\frac{1}{P^X}\|_1$ is finite, then the norm $\|V\|_1$ is finite, with division being element-wise.

Proof Property (i) comes from the definition: $(P^X)^{\text{tr}}V = \sum_{i \in \text{supp}(X)} P_i^{X_{s_0}} - P_i^{X_{s_1}} = 0$. See Appendix C for details. ■

3.3 Partial Repair

The projection in Definition 4 consist of changing the features and weights of samples in source data, while practical implementation may necessitate maintaining data distortion levels, i.e., the inner product $\langle C, \gamma \rangle$, within predefined acceptable thresholds. From a practical point of view, we consider partial repair, as relaxations of the constraint in Theorem 7.

To measure how much we violate the total repair property, we first introduce:

Definition 9 (Total variation distance (abbr. TV distance)) Given two discrete probability distributions P, Q over $\text{supp}(\tilde{X})$, the TV distance $\text{TV}(P, Q)$ between P and Q is defined as:

$$\text{TV}(P, Q) := \frac{1}{2} \sum_{j \in \text{supp}(\tilde{X})} |P_j - Q_j| = \frac{1}{2} \|P - Q\|_1. \quad (18)$$

Now let us analyse the TV distance between $P^{\tilde{X}_{s_0}}$ and $P^{\tilde{X}_{s_1}}$:

Lemma 10 Let the vector V have finite l_1 -norm, such that we can find a nonnegative vector $\Theta \in \mathbb{R}_+^N$ that satisfies

$$\Theta_j \leq \sum_{i \in \overline{\text{supp}(X)}} \gamma_{i,j} V_i \leq \Theta_j, \quad \forall j \in \text{supp}(\tilde{X}), \quad (19)$$

where $\overline{\text{supp}(X)} := \{i \in \text{supp}(X) \mid V_i \neq 0\}$. Hence, $\|\gamma^{\text{tr}}V\|_1$ is bounded by $\|\Theta\|_1$. Using Definition 9, the TV distance between $P^{\tilde{X}_{s_0}}$ and $P^{\tilde{X}_{s_1}}$ is bounded by

$$\text{TV}\left(P^{\tilde{X}_{s_0}}, P^{\tilde{X}_{s_1}}\right) = \frac{\|\gamma^{\text{tr}}V\|_1}{2} \leq \frac{\|\Theta\|_1}{2}. \quad (20)$$

Proof Equation (16) shows that $P^{\tilde{X}_0} - P^{\tilde{X}_1} = \gamma^{\text{tr}}V$. See Appendix D for details. ■

Now, we give the definition of partial repair:

Definition 11 (Partial repair) We say that Θ -repair is satisfied if $\Theta \in \mathbb{R}_+^N$, and

$$\text{TV} \left(P^{\tilde{X}_{s_0}}, P^{\tilde{X}_{s_1}} \right) \leq \frac{\|\Theta\|_1}{2}. \quad (21)$$

Note that $\mathbb{0}$ -repair is equivalent to total repair. Also, computing the value of the upper bound needs to consider the dimension of Θ , i.e., N .

3.4 Formulations and algorithms

Lemma 10 implies that in the standard formulation of regularised OT, if we were able to add the extra constraint that limits $\|\gamma^{\text{tr}}V\|_1 \leq \|\Theta\|_1$, this optimal solution γ^* would achieve Θ -repair or total repair if $\Theta = \mathbb{0}$. The revised formulation reads:

$$\inf_{\gamma \in \Pi(P^X, P^{\tilde{X}})} \left\{ \langle C, \gamma \rangle - \epsilon E(\gamma) \mid -\Theta_j \leq \sum_{i \in \text{supp}(X)} \gamma_{i,j} V_i \leq \Theta_j, \forall j \in \text{supp}(\tilde{X}) \right\}, \quad (22)$$

where $\epsilon > 0$ and $\Theta \in \mathbb{R}_+^N$.

Lemma 12 (The feasible set is non-empty) We define a subset of all admissible couplings in Equation (22):

$$\Pi_{\Theta}(P^X, P^{\tilde{X}}) := \{ \gamma \in \Sigma_N^2 \mid \gamma \mathbb{1} = P^X, \gamma^{\text{tr}} \mathbb{1} = P^{\tilde{X}}, |\gamma^{\text{tr}}V|_j \leq \Theta_j, \forall j \in \text{supp}(\tilde{X}) \}, \quad (23)$$

where $|\gamma^{\text{tr}}V|_j := \left| \sum_{i \in \text{supp}(X)} \gamma_{i,j} V_i \right|$. Let $0 \leq \Theta'_j \leq \Theta_j$ for all $j \in \text{supp}(\tilde{X})$, the following sequence holds

$$\emptyset \neq \Pi_{\mathbb{0}}(P^X, P^{\tilde{X}}) \subseteq \Pi_{\Theta'}(P^X, P^{\tilde{X}}) \subseteq \Pi_{\Theta}(P^X, P^{\tilde{X}}) \subseteq \Pi(P^X, P^{\tilde{X}}). \quad (24)$$

Therefore, the solutions of our formulation in Equation (22) exist.

Proof Remark 2.13 in Peyré et al. (2019) states that $\Pi(P^X, P^{\tilde{X}})$ is not empty because the coupling $P^X \otimes P^{\tilde{X}} \in \Pi(P^X, P^{\tilde{X}})$, where \otimes is outer product. Using Property (i) in Remark 8, we show that this coupling $P^X \otimes P^{\tilde{X}} \in \Pi_{\mathbb{0}}(P^X, P^{\tilde{X}})$. See Appendix E. \blacksquare

According to Lemma 12, and the same reasoning in Equation (7), we can rewrite Equation (22) into

$$\min_{\gamma \in \Pi_{\Theta}(P^X, P^{\tilde{X}})} \text{KL}(\gamma \parallel \xi), \text{ where } \xi = \exp(-C/\epsilon), \quad (25)$$

and $\Pi_{\Theta}(P^X, P^{\tilde{X}}) = \bigcap_{\ell=1}^3 \mathcal{C}_{\ell}$ is the intersection of three convex sets:

$$\begin{aligned} \mathcal{C}_1 &= \{ \gamma \in \mathbb{R}_+^{N \times N} \mid \gamma \mathbb{1} = P^X \}, \mathcal{C}_2 = \{ \gamma \in \mathbb{R}_+^{N \times N} \mid \gamma^{\text{tr}} \mathbb{1} = P^{\tilde{X}} \}, \\ \mathcal{C}_3 &= \{ \gamma \in \mathbb{R}_+^{N \times N} \mid -\Theta \leq \gamma^{\text{tr}}V \leq \Theta \}. \end{aligned} \quad (26)$$

Note that \mathcal{C}_3 is equivalent to $\{\gamma \in \mathbb{R}_+^{N \times N} \mid \gamma^{\text{tr}} V = \mathbf{0}\}$ if $\Theta = \mathbf{0}$.

Then apply Dykstra's algorithm, we propose Algorithm 1 to solve Equations (25-26). The inputs consist of the support $\text{supp}(X)$ (resp. $\text{supp}(\tilde{X})$) and probability distribution P^X (resp. $P^{\tilde{X}}$) of variables X (resp. \tilde{X}); the number of discretised point of these supports N ; the vectors V, Θ ; the cost matrix C ; entropic regularisation parameter $\epsilon > 0$ and the number of iterations K . The algorithm is repeated KL projections to $\mathcal{C}_1, \mathcal{C}_3, \mathcal{C}_3$, together with the computation of an auxiliary sequence $\{q_k\}_{k \geq 1}$.

Algorithm 1 Our method

Input: $\text{supp}(X), \text{supp}(\tilde{X}), N$.

Input: $P^X, P^{\tilde{X}}, V, \Theta, \epsilon, C, K$.

Define three convex sets

$$\mathcal{C}_1 = \{\gamma \in \mathbb{R}_+^{N \times N} \mid \gamma \mathbb{1} = P^X\}, \mathcal{C}_2 = \{\gamma \in \mathbb{R}_+^{N \times N} \mid \gamma^{\text{tr}} \mathbb{1} = P^{\tilde{X}}\},$$

$$\mathcal{C}_3 = \{\gamma \in \mathbb{R}_+^{N \times N} \mid -\Theta \leq \gamma^{\text{tr}} V \leq \Theta\}$$

Initialise $\gamma^{(0)} = \exp(-C/\epsilon)$

▷ Dykstra's Algorithm

for $k = 1, \dots, 3$ **do**

 Compute $\gamma^{(k)} = \mathcal{P}_{\mathcal{C}_k}^{KL}(\gamma^{(k-1)})$.

end for

for $k = 4, \dots, K$ **do**

 Set $\mathcal{C}_k = \mathcal{C}_{1+(k \bmod 3)}$

 Compute

$$q_{k-3} := \begin{cases} \frac{\gamma^{(k-4)}}{\gamma^{(k-3)}} & \text{if } k = 4, \dots, 7 \\ q_{k-7} \odot \frac{\gamma^{(k-4)}}{\gamma^{(k-3)}} & \text{otherwise.} \end{cases}$$

 Compute $\gamma^{(k)} = \mathcal{P}_{\mathcal{C}_k}^{KL}(\gamma^{(k-1)} \odot q_{k-3})$, using Lemma 14 and 15.

end for

Output: The solution of Equations (25-26): $\gamma^{(K)}$.

Now, we explain how to compute these KL projections in our algorithm:

Assumption 1 (Finite l_1 norm) *The norm $\|\frac{1}{P^X}\|_1$ is finite, where the division operator is element-wise. Then, property (iii) in Remark 8 shows that the vector V has finite l_1 -norm without infinite entries.*

Lemma 13 (Subgradient optimality conditions of KL projections) *For a set \mathcal{C} in $\mathbb{R}^{N \times N}$, we define its indicator function $\iota_{\mathcal{C}}$:*

$$\iota_{\mathcal{C}}(x) := \begin{cases} 0 & \text{if } x \in \mathcal{C}, \\ +\infty & \text{otherwise.} \end{cases} \quad (27)$$

If \mathcal{C} is a closed convex set, the KL projection for \mathcal{C} has a unique solution γ^ :*

$$\mathbf{0} \in \log\left(\frac{\gamma^*}{\bar{\gamma}}\right) + \partial \iota_{\mathcal{C}}(\gamma^*), \quad (28)$$

where $\partial\iota_{\mathcal{C}}(\gamma^*)$ denotes the set of all subgradients ν of $\iota_{\mathcal{C}}$ at $\gamma^* \in \text{dom } \iota_{\mathcal{C}}$ satisfying Equation (29), with “dom” being the essential domain:

$$\iota_{\mathcal{C}}(\gamma) \geq \iota_{\mathcal{C}}(\gamma^*) + \langle \nu, (\gamma - \gamma^*) \rangle, \forall \gamma \in \mathbb{R}^{N \times N}. \quad (29)$$

Proof See Appendix F. ■

Lemma 14 (KL projections for $\mathcal{C}_1, \mathcal{C}_2$) The KL projection for $\mathcal{C}_1, \mathcal{C}_2$ in Algorithm 1, 2 or 3 could be computed in closed form:

$$\mathcal{P}_{\mathcal{C}}^{KL}(\bar{\gamma}) = \begin{cases} \text{diag}\left(\frac{P^X}{\bar{\gamma}\mathbb{1}}\right)\bar{\gamma} & \text{if } \mathcal{C} = \{\gamma \in \mathbb{R}_+^{N \times N} \mid \gamma\mathbb{1} = P^X\}, \\ \bar{\gamma} \text{diag}\left(\frac{P^{\tilde{X}}}{\bar{\gamma}^{\text{tr}}\mathbb{1}}\right) & \text{if } \mathcal{C} = \{\gamma \in \mathbb{R}_+^{N \times N} \mid \gamma^{\text{tr}}\mathbb{1} = P^{\tilde{X}}\}, \end{cases} \quad (30)$$

where the division operator is element-wise.

Proof See Appendix G. ■

Lemma 15 (KL projections for \mathcal{C}_3) Under Assumption 1, the KL projection for \mathcal{C}_3 in Algorithm 1 could be computed in iterative manner:

$$\gamma^* = \mathcal{P}_{\mathcal{C}}^{KL}(\bar{\gamma}), \text{ where } \mathcal{C} = \left\{ \gamma \in \mathbb{R}_+^{N \times N} \mid -\Theta \leq \gamma^{\text{tr}}V \leq \Theta \right\}. \quad (31)$$

If $\bar{\gamma} \in \mathcal{C}$, $\gamma^* = \bar{\gamma}$. Otherwise, for all $i \in \text{supp}(X), j \in \text{supp}(\tilde{X})$

$$\gamma_{i,j}^* := \begin{cases} \bar{\gamma}_{i,j} \exp(-V_i \nu_j) & \text{if } i \in \overline{\text{supp}(X)} \text{ and } [\bar{\gamma}^{\text{tr}}V]_j \notin [-\Theta_j, \Theta_j], \\ \bar{\gamma}_{i,j} & \text{if } i \notin \overline{\text{supp}(X)} \text{ or } [\bar{\gamma}^{\text{tr}}V]_j \in [-\Theta_j, \Theta_j]. \end{cases} \quad (32)$$

where $[\bar{\gamma}^{\text{tr}}V]_j$ is the j^{th} entry of the vector $\bar{\gamma}^{\text{tr}}V$. ν_j needs to satisfy Equation (33). The computation and existence of ν_j are in Remark 16.

$$\sum_{i \in \overline{\text{supp}(X)}} \bar{\gamma}_{i,j} V_i \exp(-V_i \nu_j) = \begin{cases} \Theta_j & \text{if } [\bar{\gamma}^{\text{tr}}V]_j > \Theta_j, \\ -\Theta_j & \text{if } [\bar{\gamma}^{\text{tr}}V]_j < -\Theta_j. \end{cases} \quad (33)$$

Proof See Appendix H. ■

Remark 16 (Computation and existence of ν_j) ν_j in Equation (33) is indeed the root of function $F(x) := \sum_{i \in \overline{\text{supp}(X)}} \bar{\gamma}_{i,j} V_i \exp(-V_i x) + c$, where $c = \pm\Theta_j$ is a constant. Its first derivative $\nabla F(x) = -\sum_{i \in \overline{\text{supp}(X)}} \bar{\gamma}_{i,j} (V_i)^2 \exp(-V_i x) \leq 0$, such that $F(x)$ is non-increasing. Under Assumption 1, the root (i.e., ν_j) can be found by root-finding algorithms e.g., Newton-Raphson algorithm, bisection method. See Appendix I for existence of the root.

Lemma 17 (Convergence of Algorithm 1) *In the case of binary sensitive attributes, i.e., $\text{supp}(S) = \{s_0, s_1\}$, under Assumption 1, given the vector $\Theta \in \mathbb{R}_+^N$, and KL projections being computed as in Lemma 14-15, Algorithm 1 converges to the unique coupling of Equation (25-26). Then projecting the source data via the group-blind map induced from the unique coupling, we can achieve Θ -repair in projected data.*

Proof *This proof relies on computation of KL projections, which is explained in Lemma 13-15, and the convergence result of Dykstra’s algorithm which is explained in Appendix J, with Lemma 12 ensuring that our formulation satisfies the assumption of Dykstra’s algorithm. ■*

3.5 Higher dimensions

Now, we consider situations with more than one unprotected attribute:

- There are extra attribute(s) $U \in \mathbb{R}^d, d \geq 1$ in the source data that need to stay the same during the projection, or U is S -neutral. In this case, a sample becomes (i, u, s) , where $i \in \text{supp}(X)$, and u, s are the values of attributes U, S . As mentioned in Definition 4, the projection map \mathcal{T} would not change any attributes other than X . Hence, this sample is split into a sequence of weighted samples $\{(j, w_j, u, s)\}_{j \in \text{supp}(\tilde{X})}$.
- There are extra attribute(s) that need to be adjusted. Without loss of generality, we assume attributes $X_1, X_2 \in \mathbb{R}$ need to be adjusted. Let $X = (X_1, X_2)$ and $\text{supp}(X) = \text{supp}((X_1, X_2)) \in \mathbb{R}^2$, such that $\text{supp}(X)$ includes all tuples (x_1, x_2) present in the source data, where $x_1 \in \text{supp}(X)_1, x_2 \in \text{supp}(X)_2$. Then N is the cardinality of the set $\text{supp}(X)$. In the same manner, we can define $\text{supp}(\tilde{X})$ and the probability distributions:

$$\begin{aligned} P_i^X &:= \Pr[(X_1, X_2) = i], & P_i^{X_s} &:= \Pr[(X_1, X_2) = i \mid S = s], \forall i \in \text{supp}(X), \\ P_j^{\tilde{X}} &:= \Pr[(\tilde{X}_1, \tilde{X}_2) = j], & P_j^{\tilde{X}_s} &:= \Pr[(\tilde{X}_1, \tilde{X}_2) = j \mid S = s], \forall j \in \text{supp}(\tilde{X}). \end{aligned} \quad (34)$$

It is worth noting that the cost matrix C needs to consider the range of each attribute that need to be adjusted. Suppose $\text{supp}(X_1) = \{1, 2\}$ and $\text{supp}(X_2) = \{1, \dots, 4\}$. While not necessarily appropriate in practice, if the entries of cost matrix $C_{i,j} := \|i - j\|_1$, the cost of moving X_1 from 1 to 2 would be treated the same as moving X_2 from 1 to 2. Instead, we use $C_{i,j} := \|g \odot (i - j)\|_1$, where $g \in \mathbb{R}_+^2$ denotes the weights for the cost of moving one unit of X_1, X_2 , and \odot is element-wise product. If $g = [1, 1/4]$, the cost of moving X_1 from 1 to 2 is the same as moving X_2 from 1 to 4.

3.6 Choices of target distributions

There is no an explicit requirement regarding $P^{\tilde{X}} \in \Sigma_N$ in Lemma 17. It leaves the choice of target distribution open.

- Concerning with data distortion, one option would be the barycentre distribution, because it brings the least alteration to source data, from its definition in Equation (38), or in the original works of Gordaliza et al. (2019); Oneto and Chiappa (2020); Jiang et al. (2020). In our setting, the requirement regarding the sensitive attribute S is

the vector V only. If those S -wise distributions $P^{X_{s_0}}, P^{X_{s_1}}$ are not explicitly given, we cannot compute the barycentre between them. But we include it as barycentre baseline in Section 4.2.

- The other option concerns with performance or utility of some pre-established machine learning models. Suppose the classification or prediction model is trained on a training set. We set the target distribution the same as the the distribution of the training set, or other common representation space, to preserve the classification or prediction performance of the pre-trained model.

4 Numerical Illustrations

Repair schemes consist of mapping source data into the pre-designed target data, and after the mapping, we obtain the projected data, which are expected to have equalised distributions of features in privileged and unprivileged groups. During the mapping, a sample in the source data is divided into a sequence of weighted samples, leading to data distortion—specifically, a deviation from its original representation. The data distortion may dampen accuracy or utility of some pre-trained prediction or classification models. For example, recall the motivating example introduced in Section 1.1. If all applicants are projected to the maximum exam score, the cut-off point loses its ability to distinguish between privileged and unprivileged groups but also significantly forfeits its capacity to classify qualified applicants.

This section first demonstrates the effects of our total repair and partial repair schemes using synthetic data, and then illustrates the classic trade-off between bias repair and data distortion, using the adult census dataset of Becker and Kohavi (1996). Specifically, Section 4.1 explains how we use the sensitive attribute in experiments and introduce the performance indices. Section 4.2 introduces two baselines. Sections 4.3 and 4.4 describe our experiments on synthetic data and real data, with comparison with these baselines. Our implementation is available online ¹.

4.1 Input and Indices

We have made the assumption that the sensitive attribute S of each sample is not observed, but the vector V , as defined in Theorem 7, is given as the input for our algorithm. The computation of V requires the population-level information regarding the distributions of features for both groups (s_0 and s_1), given the crucial assumption that the source data represents unbiased samples from the broader population, such that groups in source data follow the same distributions. In our experiments, since there is no such population-level information given, we directly compute V from the source data. Apart from computing V , the sensitive attribute of each sample is not utilised for computing the coupling or for projecting source data.

Next, to introduce the performance indices, we start from defining computation of empirical distributions:

1. https://github.com/Quan-Zhou/OT_Debiasing

Definition 18 (Empirical distributions) Let $\text{supp}(Z) \in \mathbb{R}$. Given data $(i, w_i)_{i \in \text{supp}(Z)}$, the empirical distribution P^Z is defined as

$$P_i^Z := \frac{w_i}{\sum_{i \in \text{supp}(Z)} w_i}. \quad (35)$$

For instance, Equation (35) computes P^X if $Z = X$, and $P^{\tilde{X}}$ if $Z = \tilde{X}$. If the sensitive attribute S is known, such that the data become $(i, s, w_{i,s})_{i \in \text{supp}(Z), s \in \text{supp}(S)}$, we can compute the S -wise distributions P^{Z_s} as follows:

$$P_i^{Z_s} := \frac{w_{i,s}}{\sum_{i \in \text{supp}(Z)} w_{i,s}}, \quad \forall s \in \text{supp}(S). \quad (36)$$

Definition 19 (Performance indices) Let Y and f denote the label that we need to estimate and the estimated label. To measure the performance of prediction / classification models on the source or projected data, we introduce f1 scores as accuracy measures, disparate impact as the fairness measure, and S -wise TV distance:

$$\begin{aligned} f1 \text{ micro} &:= \frac{\sum_{s \in \text{supp}(S)} (2 \times TP_s)}{\sum_{s \in \text{supp}(S)} (2 \times TP_s + FP_s + FN_s)}, \\ f1 \text{ macro} &:= \sum_{s \in \text{supp}(S)} \frac{1}{2} \times \frac{2 \times TP_s}{2 \times TP_s + FP_s + FN_s}, \\ f1 \text{ weighted} &:= \sum_{s \in \text{supp}(S)} P_s^S \times \frac{2 \times TP_s}{2 \times TP_s + FP_s + FN_s}, \\ \text{DisparateImpact} &:= \frac{\Pr[f = 1 \mid S = s_0]}{\Pr[f = 1 \mid S = s_1]}, \\ S\text{-wise TV distance} &:= \text{TV}(P^{\tilde{X}_{s_0}}, P^{\tilde{X}_{s_1}}), \end{aligned}$$

where s_0 denotes the unprivileged group and $Y = 0$ is the negative label. TP_s, FP_s, FN_s are the numbers of true positive, false positive and false negative of the group s . Empirical distributions $P^S, P^{\tilde{X}_{s_0}}, P^{\tilde{X}_{s_1}}$ are computed from the projected data, following Definition 18. Ideally, after the repair, f1 scores increase, disparate impact gets closer to 1, and S -wise TV distance decreases.

4.2 Two baselines

Definition 20 (The baseline of iterative Bregman projections) The first baseline is to solve the standard regularised OT formulation:

$$\min_{\gamma \in \Pi(P^X, P^{\tilde{X}})} \langle C, \gamma \rangle - \epsilon E(\gamma) = \text{KL}(\gamma \parallel \xi), \quad \text{where } \Pi(P^X, P^{\tilde{X}}) = \bigcap_{\ell=1}^2 \mathcal{C}_\ell, \quad \xi = \exp(-C/\epsilon). \quad (37)$$

The only difference between the baseline and our method is that we add one additional constraint $-\Theta \leq \gamma^{\text{tr}} V \leq \Theta$. The optimal solution of Equation (37) can be founded by Dykstra's Algorithm, or computationally cheaply using the iterative Bregman projections,

as suggested in Algorithm 2. Both algorithms converge at the same results, because $\mathcal{C}_1, \mathcal{C}_2$ are affine subspaces (See Fact 1.4 in Bauschke et al. (2020), or Theorem 4.3 in Bauschke and Lewis (2000)).

Algorithm 2 Baseline method

Input: $\text{supp}(X), \text{supp}(\tilde{X}), N, P^X, P^{\tilde{X}}, \epsilon, C, K$.

Set

$$\mathcal{C}_1 = \{\gamma \in \mathbb{R}_+^{N \times N} \mid \gamma \mathbb{1} = P^X\}, \quad \mathcal{C}_2 = \{\gamma \in \mathbb{R}_+^{N \times N} \mid \gamma^{\text{tr}} \mathbb{1} = P^{\tilde{X}}\}.$$

Initialise $\gamma^{(0)} = \exp(-C/\epsilon)$.

▷ Iterative Bregman Projections

for $k = 1, \dots, K$ **do**

Set $\mathcal{C}_k = \mathcal{C}_{1+(k \bmod 2)}$

Compute $\gamma^{(k)} = \mathcal{P}_{\mathcal{C}_k}^{KL}(\gamma^{(k-1)})$, using Lemma 14.

end for

Output: The solution of Equation (37): $\gamma^{(K)}$.

We consider another baseline of barycentre projection:

Definition 21 (The barycentre projection in Gordaliza et al. (2019)) *The second baseline is the total repair in Section 5.1.1 (B) of Gordaliza et al. (2019), where each sample split its mass to be transported, the same as our setting. The idea is that the two conditional distributions of the random variable X by the protected attribute S are going to be transformed into the Wasserstein barycentre P^B between $P^{X_{s_0}}$ and $P^{X_{s_1}}$, with weight π_0 and π_1 . The 1-Wasserstein barycentre is defined as*

$$P^B = \arg \min_{P \in \Sigma_N} \{\pi_0 \mathcal{W}_1(P^{X_{s_0}}, P) + \pi_1 \mathcal{W}_1(P^{X_{s_1}}, P)\}, \quad (38)$$

where $\mathcal{W}_1(P^{X_{s_0}}, P^{X_{s_1}}) := \sum_{i \in \text{supp}(X)} |P_i^{X_{s_0}} - P_i^{X_{s_1}}|$ denotes the 1-Wasserstein distance between two distributions $P^{X_{s_0}}, P^{X_{s_1}}$ defined on $\text{supp}(X)$. The nonnegative constants $\pi_0 + \pi_1 = 1$ are barycentric coordinates.

The barycentre within two marginal distributions can be found via the optimal coupling between $P^{X_{s_0}}, P^{X_{s_1}}$ (Remark 4.1 in Gordaliza et al. (2019), or Proposition 5.9 in Villani (2021)). The implementation is to find the coupling $\gamma^B \in \Pi(P^{X_{s_0}}, P^{X_{s_1}})$, as in Algorithm 3, and then transport the group of s_0 by the map corresponding to the coupling $\gamma^{0 \rightarrow B}$ and the group of s_1 by the map corresponding to the coupling $\gamma^{1 \rightarrow B}$, whose entries are defined by

$$\gamma_{i,k}^{0 \rightarrow B} := \gamma_{i, \pi_0 \cdot i + \pi_1 \cdot k}^B, \quad \gamma_{i,k}^{1 \rightarrow B} := \gamma_{\pi_1 \cdot i + \pi_0 \cdot k, i}^B. \quad (39)$$

Algorithm 3 Barycentre method

Input: $\text{supp}(X), N, P^{X_{s_0}}, P^{X_{s_1}}, \epsilon, C, K, \pi_0, \pi_1$.

Set

$$\mathcal{C}_1 = \{\gamma \in \mathbb{R}_+^{N \times N} \mid \gamma \mathbf{1} = P^{X_{s_0}}\}, \mathcal{C}_2 = \{\gamma \in \mathbb{R}_+^{N \times N} \mid \gamma^{\text{tr}} \mathbf{1} = P^{X_{s_1}}\}.$$

Initialise $\gamma^{(0)} = \exp(-C/\epsilon)$.

▷ Iterative Bregman Projections

for $k = 1, \dots, K$ **do**

Set $\mathcal{C}_k = \mathcal{C}_{1+(k \bmod 2)}$

Compute $\gamma^{(k)} = \mathcal{P}_{\mathcal{C}_k}^{KL}(\gamma^{(k-1)})$, using Lemma 14.

end for

Output: The solution of γ^B in Definition 21: $\gamma^{(K)}$.

4.3 Revisiting the motivating example

In the first example, we compare with the baseline in Definition 20 on synthetic data, to demonstrate that an arbitrary S -blind projection map would not reach total repair.

Recall the motivating example introduced in Section 1.1, where there is only one unprotected attribute (the exam score) and one binary sensitive attribute. Let $\text{supp}(X) = \text{supp}(\tilde{X}) = \{-30, -29, \dots, 10\}$. Suppose $\text{supp}(S) = \{s_0, s_1\}$ and $\Pr[s_0] = 0.7, \Pr[s_1] = 0.3$. The random variable X_{s_0} (resp. X_{s_1}) follow a discretised Gaussian distribution $\mathcal{N}(-10, 6^2)$ (resp. $\mathcal{N}(1, 3^2)$).

We generate $M = 10^4$ samples (source data) by repeating the procedure for M times: first, we generate a uniform random variable within $[0, 1]$. If this uniform variable is smaller than $\Pr[s_0]$, we generate a Gaussian random variable $X_{s_0} \sim \mathcal{N}(-10, 6^2)$ and the sample reads $(\lfloor X_{s_0} \rfloor, s_0)$, where $\lfloor \cdot \rfloor$ is the floor function. Otherwise, the sample should be $(\lfloor X_{s_1} \rfloor, s_1)$, where $X_{s_1} \sim \mathcal{N}(1, 3^2)$. Then, we compute the empirical distributions of $P^X, P^{X_{s_0}}, P^{X_{s_1}}, P^S$ from the source data. For the target distribution, we arbitrarily set $P^{\tilde{X}}$ to the distribution of discretised Gaussian distribution $\mathcal{N}(-5, 5^2)$. In Figure 2, the discrete distributions $P^X, P^{X_{s_0}}, P^{X_{s_1}}, P^{\tilde{X}}$ are displayed by blue, orange, purple, green curves, respectively.

Compute $V = (P^{X_{s_0}} - P^{X_{s_1}})/P^X$, set the entry of cost matrix $C_{i,j} = |i - j|$, $\epsilon = 0.01$ and the number of iteration $K = 400$ for baseline and $K = 600$ for our method. Along with $P^X, P^{\tilde{X}}, V, \epsilon, C, K$ and $\Theta = 10^{-2}\mathbf{1}, 10^{-3}\mathbf{1}, \mathbf{0}$ as input in Algorithm 1, we find the optimal coupling γ^* of Equations (25-26) and another baseline coupling of Equation (37), shown in Figure 3, where the blue and green curves represent P^X and $P^{\tilde{X}}$.

Then, for each coupling, we define a projection map following Definition 4. After applying the projections to source data, we compute the empirical distributions of $P^{\tilde{X}_{s_0}}$ and $P^{\tilde{X}_{s_1}}$ from the projected data. In Figure 5, from left to right, we show the S -wise empirical distributions of source data, projected data from baseline, from $10^{-2}\mathbf{1}$ -repair, from $10^{-3}\mathbf{1}$ -repair, and from total repair, with $P^{\tilde{X}_{s_0}}$ plotted orange and $P^{\tilde{X}_{s_1}}$ plotted purple. We can see that when Θ gets closer to $\mathbf{0}$, the gap between purple and orange curves shrinks.

In order to demonstrate that all couplings in Figure 3 are feasible, we present the empirical $P^{\tilde{X}}$ (dashed green curves) computed from projected data and the input of target distribution $P^{\tilde{X}}$ used to compute all couplings (solid green curves) in Figure 4. The overlap

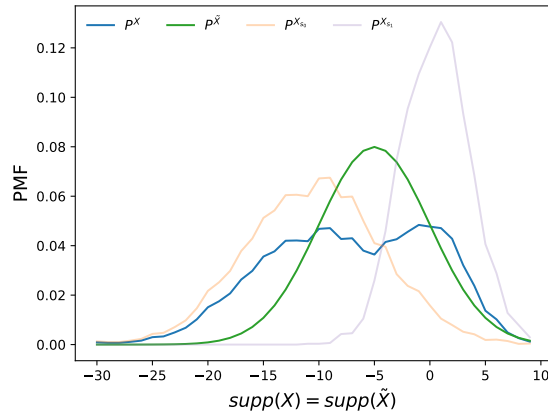


Figure 2: Overview of the empirical distributions of $P^X, P^{X_{s_0}}, P^{X_{s_1}}$ from the generated source data and the target distribution $P^{\tilde{X}}$ that we set arbitrarily.

of both green curves implies that source data are successfully projected to the target data we expect, regardless of the coupling used.

4.4 A trade-off between bias repair and data distortion

We conduct random-forest classification models on the adult census dataset in Becker and Kohavi (1996), to showcase the trade-off between bias repair and data distortion, compared with the total repair using barycentre projection in Gordaliza et al. (2019).

The adult census dataset (Becker and Kohavi, 1996) comprises of 48842 samples of 14 features (e.g., gender, race, age, education level, marital-status, occupation) and a high-income indicator. The high-income indicator denotes whether the annual income of a sample is lower than \$50K (label $Y = 0$) or higher (label $Y = 1$). There are five numerical features out of these 14 features: “education level” (ranging from 1 to 16) and “hours per week”, “age”, “capital gain”, “capital loss” (ranging from 0 to 4). There are two commonly-recognised sensitive attributes, i.e., “race” and “sex”.

If the sensitive attribute S is “race”, we select all samples ($M = 46447$) whose race is black ($S = 0$) or white ($S = 1$). If S is “sex”, we select all samples ($M = 48842$) whose gender is female ($S = 0$) or male ($S = 1$). For each numerical feature, we compute the total variation distance between race-wise (resp. gender-wise) marginal distributions in Table 1. They are used as reference to decide which features need to be adjusted, to avoid unnecessary alteration. We let X include all features with S -wise TV distance higher than 0.08, ensuring that only two features are selected when S represents “race” or “sex”. Specifically, X contains “education level”, “hours per week” if S is “race”, and X contains the “hours per week”, “age” if S is “sex”. The other features are considered as S -neutral and denoted as U .

We have performed 30-fold cross-validation. For each trial, we randomly select 60% of M samples as the training set, and use these five numerical features and the high income

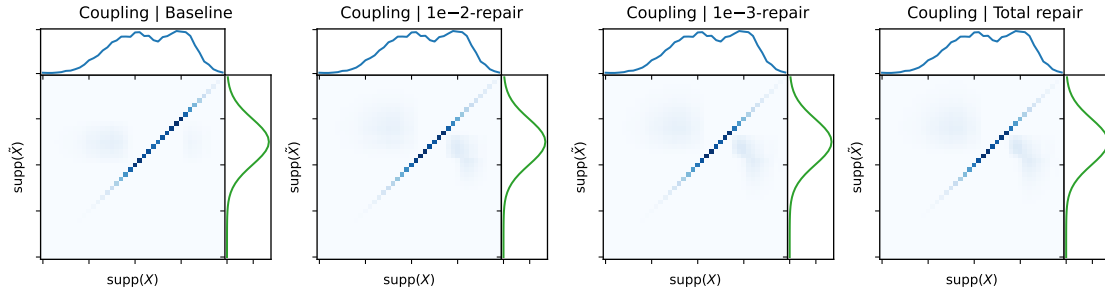


Figure 3: From left to right: the baseline coupling of Equation (37), the optimal coupling γ^* of Equations (25-26), when $\Theta = 10^{-2}\mathbf{1}, 10^{-3}\mathbf{1}, \mathbf{0}$. The blue and green curves represent marginal distributions $P^X, P^{\tilde{X}}$ that are the same across all couplings.

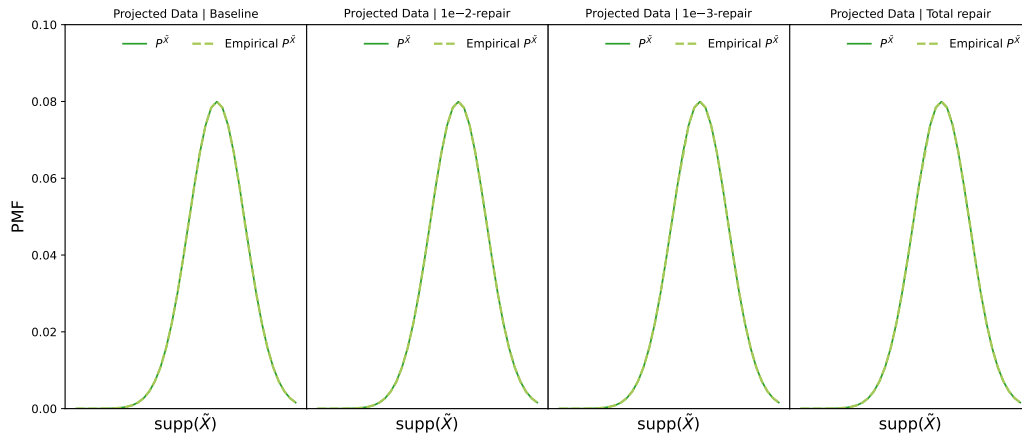


Figure 4: **Group-blind distributions.** Solid green curves are the S -blind target distributions $P^{\tilde{X}}$ used to compute couplings, which are the green curves in Figure 3. Dashed green curves (from left to right) are the S -blind empirical distributions of $P^{\tilde{X}}$ computed from projected data from baseline, from $10^{-2}\mathbf{1}$ -repair, from $10^{-3}\mathbf{1}$ -repair, and from total repair. The overlap between dashed curves and solid curves shows the projected data follow the target distribution we design, and verifies that all couplings in Figure 3 are feasible and the projection method in Definition 4 is correct.

indicator Y to build a random-forest model $\mathcal{M}(X, U)$, with the sensitive attribute S ignored. The outputs of the model $f = \mathcal{M}(X, U)$ is the prediction of Y .

The rest 40% of M samples are used as the test set. From the test set, we compute the empirical marginal distributions of the feature X (i.e., P^X, P^{X_0}, P^{X_1}) and V . Next, we handle the test set in five different ways as outlined below.

- Do nothing (denoted “Origin”).

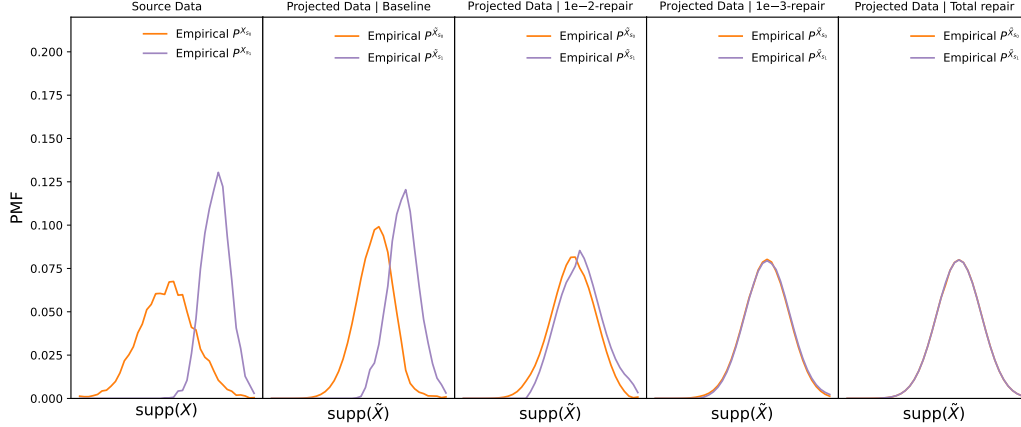


Figure 5: **Group-wise distributions.** From left to right: the S -wise empirical distributions of $P^{X_{s_0}}, P^{X_{s_1}}$ in source data, $P^{\tilde{X}_{s_0}}, P^{\tilde{X}_{s_1}}$ in projected data from baseline, from 10^{-2} -repair, from 10^{-3} -repair, and from total repair. $P^{\tilde{X}_{s_0}}$ is plotted orange and $P^{\tilde{X}_{s_1}}$ is plotted purple.

Features	Race-wise TV distance	Gender-wise TV distance
age	0.0415	0.1010
education level	0.1187	0.0710
capital gain	0.0268	0.0369
capital loss	0.0142	0.0201
hours per week	0.1222	0.1819

Table 1: The TV distance between race-wise and gender-wise marginal distributions of five numerical features in the adult census dataset (Becker and Kohavi, 1996). Highlighted features, whose S -wise TV distance higher than 0.08 are chosen as X and would be adjusted. The rest are considered as S -neutral and denoted as U .

- For each sample in test set, project its X features with a baseline coupling computed as in Definition 20 (denoted “Baseline”). The other features and Y stay the same.
- Project its X features with a barycentre coupling computed as in Definition 21 (denoted “Barycentre”). The other features and Y stay the same.
- Project its X features with a coupling computed by Algorithm 1 with $\Theta = 1e^{-2}\mathbb{1}$ (denoted “ $1e^{-2}$ -repair”). The other features and Y stay the same.
- Project its X features with a coupling computed by Algorithm 1 with $\Theta = 1e^{-3}\mathbb{1}$ (denoted “ $1e^{-3}$ -repair”). The other features and Y stay the same.

The number of iterations is $K = 400$ for “Baseline”, “Barycentre”, and is $K = 600$ for our partial repair schemes, i.e., “ $1e^{-2}$ -repair”, “ $1e^{-3}$ -repair”. The entropic regularisation parameter is $\epsilon = 0.01$. The entry of cost matrix is $C_{i,j} := \|g \odot (i-j)\|_1$, where the entry g_i is the reciprocal of the range of the i^{th} feature in X . Both source and target distributions are P^X in “Baseline” and our partial repair schemes “ $1e^{-2}$ -repair”, “ $1e^{-3}$ -repair”, such that the target distribution is simply $P^{\tilde{X}} = P^X$ to avoid unnecessary data distortion. “Barycentre” use $P^{X_{s_0}}$ as source and $P^{X_{s_1}}$ as target, with π_0 being the portion of s_0 group in source data, the same setting as in Gordaliza et al. (2019).

We test the five test sets on a random-forest classification model built from the training set as follows. Given a sample (x, u, s, y) in the test set, for “Origin”, the prediction of its high income indicator is $f = \mathcal{M}(x, u)$. With exception of “Origin”, this sample is split into a sequence of weighted samples $\{(\tilde{x}, u, s, y, w_{\tilde{x}})\}_{\tilde{x} \in \text{supp}(\tilde{X})}$. In this case, the repaired prediction would be 0 if $\sum_{\tilde{x} \in \text{supp}(\tilde{X})} w_{\tilde{x}} f^{\tilde{x}} < f_{th}$ and 1 otherwise, where the prediction for a single sample is $f^{\tilde{x}} = \mathcal{M}(\tilde{x}, u)$, and the threshold is $f_{th} = 0.1$, chosen by grid search.

Once the predictions for the five test sets are computed, we measure the performance by disparate impact, f1 scores and S -wise TV distance, as in Definition 19. Note that for “Origin”, the S -wise TV distance is $\text{TV}(P^{X_{s_0}}, P^{X_{s_1}})$. After 30 trials, where in each trial we generate new training set and test set, we can further compute the mean and standard deviation of these performance indices of each model.

In Figure 6, we present disparate impact, f1 scores and S -wise TV distance of the prediction for these five test sets as the mean (bars) and mean \pm standard deviation (dark vertical lines) across the 30 trials. To distinguish the test sets, “Origin” is plotted in brown, “Baseline” is plotted in dark red, “ $1e^{-2}$ -repair” is plotted in orange, “ $1e^{-3}$ -repair” is plotted in yellow and “Barycentre” is plotted in light red. It is expected that the S -wise TV distance of “Barycentre” is almost zero, as it is one of the total repair schemes of Gordaliza et al. (2019).

5 Conclusion

We provided new bias repair schemes to mitigate disparate impact, via the technologies of optimal transport, without access to each datapoint’s sensitive attribute. The limitation is that only one binary attribute is allowed. We could further extend these schemes to cases where the sensitive attribute has multiple classes, or extend to the accelerated Dykstra’s algorithm in Chai and Wang (2022).

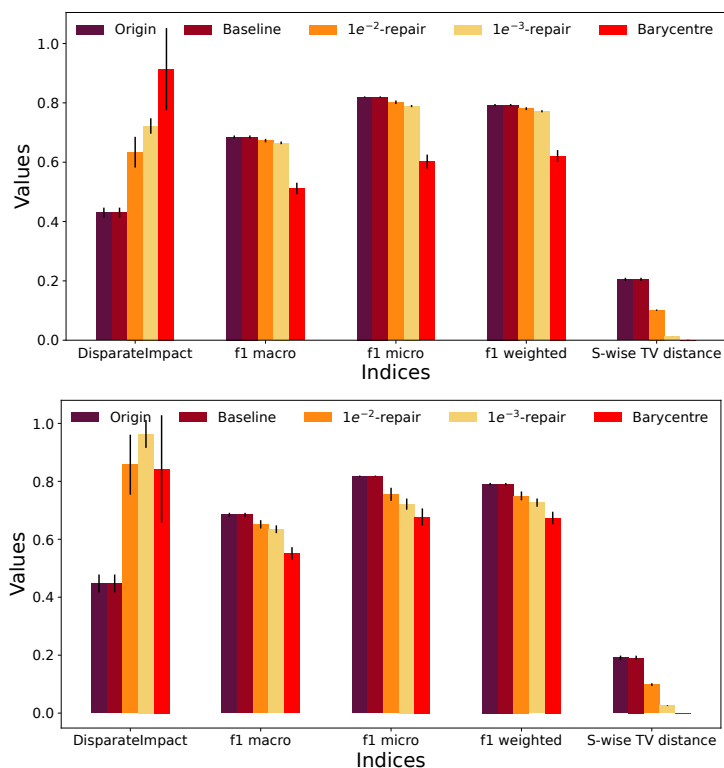


Figure 6: Prediction performance for adult census dataset Becker and Kohavi (1996), with S being “sex” (upper) and “race” (lower). The mean and mean \pm one standard deviation of these performance indices, across 30 trials are displayed by bars and dark vertical lines. ‘Origin’ method without any bias repair is plotted in brown, ‘Baseline’ is plotted in dark red, ‘Barycentre’ in Gordaliza et al. (2019) is plotted in light red. Our partial repair schemes “ $1e^{-2}$ -repair” is plotted in orange and “ $1e^{-3}$ -repair” is plotted in yellow. An ideal method should have the disparate impact close to 1, f1 scores as high as possible and S -wise TV distance close to 0.

Acknowledgments and Disclosure of Funding

We would like to acknowledge the contributions of Anthony Quinn and Robert Shorten, who suggested (Quinn et al., 2023) to work on fairness repair without the protected attribute, following discussions within the AutoFair project as to the unavailability of the protected attributes in many settings. The original contribution of Anthony Quinn and Robert Shorten was to consider “research data” (Quinn et al., 2023, Slide 23), as in a regulatory sandbox, as a means to repair data-sets with an unavailable protected attribute. This insight has been instrumental in deriving Theorem 7, which utilises marginals $P^{X_{s_0}}, P^{X_{s_1}}$ of the general population. We would also like to extend our sincere thanks to Robert Shorten for his subsequent invaluable help, including his suggestion to focus on feature distribution information via unbiased sampling from a wider population and to test the feasibility of our formulation using numerical experiments, as well as his proofreading of the manuscript. This work has been done in parallel with the work of Elzayn et al. (2023), whose pre-print appeared in arxiv on October 2nd, 2023, two weeks ahead of the present pre-print. This work has received funding from the European Union’s Horizon Europe research and innovation programme under grant agreement No. 101070568. This work was also supported by Innovate UK under the Horizon Europe Guarantee; UKRI Reference Number: 10040569 (Human-Compatible Artificial Intelligence with Guarantees (AutoFair)).

Appendix A. Proof of Lemma 6

The right equation follows from the definition of coupling, as in Equation (2). We only prove the left equation. Since the projection \mathcal{T} from X to \tilde{X} is irrelevant to S , the following holds

$$\Pr [\tilde{X} = j \mid X = i, S = s] = \Pr [\tilde{X} = j \mid X = i], \forall i \in \text{supp}(X_s). \quad (40)$$

Using Bayes theorem, for $i \in \text{supp}(X_s)$:

$$\begin{aligned} \Pr [X = i, \tilde{X} = j, S = s] &= \Pr [\tilde{X} = j \mid X = i, S = s] \Pr [X = i, S = s] \\ &= \Pr [\tilde{X} = j \mid X = i] \Pr [X = i, S = s] \\ &= \Pr [X = i, \tilde{X} = j] \frac{\Pr [X = i, S = s]}{\Pr [X = i]} \\ &= \Pr [X = i, \tilde{X} = j] \Pr [S = s \mid X = i]. \end{aligned}$$

Further,

$$\begin{aligned}
\Pr \left[\tilde{X} = j \mid S = s \right] &= \frac{\Pr \left[\tilde{X} = j, S = s \right]}{\Pr [S = s]} = \frac{\sum_{i \in \text{supp}(X_s)} \Pr \left[X = i, \tilde{X} = j, S = s \right]}{\Pr [S = s]} \\
&= \frac{\sum_{i \in \text{supp}(X_s)} \Pr \left[X = i, \tilde{X} = j \right] \Pr [S = s \mid X = i]}{\Pr [S = s]} \\
&= \sum_{i \in \text{supp}(X_s)} \Pr \left[X = i, \tilde{X} = j \right] \frac{\Pr [S = s \mid X = i]}{\Pr [S = s]} \\
&= \sum_{i \in \text{supp}(X_s)} \Pr \left[X = i, \tilde{X} = j \right] \frac{\Pr [S = s, X = i]}{\Pr [X = i] \Pr [S = s]} \\
&= \sum_{i \in \text{supp}(X_s)} \Pr \left[X = i, \tilde{X} = j \right] \frac{\Pr [X = i \mid S = s]}{\Pr [X = i]}.
\end{aligned}$$

We obtain

$$\Pr \left[\tilde{X} = j \mid S = s \right] = \sum_{i \in \text{supp}(X_s)} \Pr \left[X = i, \tilde{X} = j \right] \frac{\Pr [X = i \mid S = s]}{\Pr [X = i]}, \forall j \in \text{supp}(\tilde{X}), s \in \text{supp}(S).$$

Note that $\Pr [X = i \mid S = s]$ is not defined on $\text{supp}(X) \setminus \text{supp}(X_s)$. If we set the undefined conditional probability be $\Pr [X = i \mid S = s] = 0$ for $i \in \text{supp}(X) \setminus \text{supp}(X_s)$, and rewrite the equation above in matrix form, we complete the proof.

Appendix B. Proof of Theorem 7

Total repair in Definition 5 requires that for $j \in \text{supp}(\tilde{X})$, the difference between $\Pr \left[\tilde{X} = j \mid s_0 \right]$ and $\Pr \left[\tilde{X} = j \mid s_1 \right]$ is zero. $\text{supp}(X)$ could be divided into three disjoint subsets: $\text{supp}(X_{s_0}) \cap \text{supp}(X_{s_1})$, $\text{supp}(X_{s_0}) \setminus \text{supp}(X_{s_1})$ and $\text{supp}(X_{s_1}) \setminus \text{supp}(X_{s_0})$. Let $\mathbb{X}^{0 \wedge 1}$, \mathbb{X}^{0-1} and \mathbb{X}^{1-0} denote these three subsets. Using Lemma 6, we deduce that

$$\begin{aligned}
&\Pr \left[\tilde{X} = j \mid s_0 \right] - \Pr \left[\tilde{X} = j \mid s_1 \right] \\
&= \sum_{i \in \text{supp}(X_{s_0})} \Pr \left[X = i, \tilde{X} = j \right] \frac{\Pr [X = i \mid S = s_0]}{\Pr [X = i]} - \sum_{i \in \text{supp}(X_{s_1})} \Pr \left[X = i, \tilde{X} = j \right] \frac{\Pr [X = i \mid S = s_1]}{\Pr [X = i]} \\
&= \sum_{i \in \mathbb{X}^{0 \wedge 1}} \Pr \left[X = i, \tilde{X} = j \right] \frac{\Pr [X = i \mid S = s_0]}{\Pr [X = i]} + \sum_{i \in \mathbb{X}^{0-1}} \Pr \left[X = i, \tilde{X} = j \right] \frac{\Pr [X = i \mid S = s_0]}{\Pr [X = i]} \\
&\quad - \sum_{i \in \mathbb{X}^{0 \wedge 1}} \Pr \left[X = i, \tilde{X} = j \right] \frac{\Pr [X = i \mid S = s_1]}{\Pr [X = i]} - \sum_{i \in \mathbb{X}^{1-0}} \Pr \left[X = i, \tilde{X} = j \right] \frac{\Pr [X = i \mid S = s_1]}{\Pr [X = i]} \\
&= \sum_{i \in \mathbb{X}^{0 \wedge 1}} \Pr \left[X = i, \tilde{X} = j \right] \frac{\Pr [X = i \mid S = s_0] - \Pr [X = i \mid S = s_1]}{\Pr [X = i]} \\
&\quad + \sum_{i \in \mathbb{X}^{0-1}} \Pr \left[X = i, \tilde{X} = j \right] \frac{\Pr [X = i \mid S = s_0]}{\Pr [X = i]} - \sum_{i \in \mathbb{X}^{1-0}} \Pr \left[X = i, \tilde{X} = j \right] \frac{\Pr [X = i \mid S = s_1]}{\Pr [X = i]}.
\end{aligned}$$

Hence, if we want to achieve total repair, the coupling γ must satisfy for $j \in \text{supp}(\tilde{X})$

$$\begin{aligned}
0 &= \sum_{i \in \mathbb{X}^{0 \wedge 1}} \Pr \left[X = i, \tilde{X} = j \right] \frac{\Pr[X = i | S = s_0] - \Pr[X = i | S = s_1]}{\Pr[X = i]} \\
&+ \sum_{i \in \mathbb{X}^{0-1}} \Pr \left[X = i, \tilde{X} = j \right] \frac{\Pr[X = i | S = s_0]}{\Pr[X = i]} - \sum_{i \in \mathbb{X}^{1-0}} \Pr \left[X = i, \tilde{X} = j \right] \frac{\Pr[X = i | S = s_1]}{\Pr[X = i]}.
\end{aligned} \tag{41}$$

Note that $\Pr[X = i | S = s]$ is not defined on $\text{supp}(X) \setminus \text{supp}(X_s)$. Now, set $\Pr[X = i | S = s_0] = 0$ for $i \in \mathbb{X}^{1-0}$ and $\Pr[X = i | S = s_1] = 0$ for $i \in \mathbb{X}^{0-1}$, such that for all $i \in \text{supp}(X)$, it holds $\Pr[X = i] > 0$ and $\Pr[X = i | S = s] \geq 0$ for $x \in \text{supp}(X), s \in \text{supp}(S)$. Equation (41) can be simplified into

$$\sum_{i \in \text{supp}(X)} \Pr \left[X = i, \tilde{X} = j \right] \frac{\Pr[X = i | S = s_0] - \Pr[X = i | S = s_1]}{\Pr[X = i]} = 0, \forall j \in \text{supp}(\tilde{X}). \tag{42}$$

Rewrite it into the matrix form. Using the definition of the vector V , Equation (42) is further simplified into

$$\gamma^{\text{tr}} V = \mathbf{0}. \tag{43}$$

Appendix C. Proof of properties in Remark 8

Since we have defined the conditional probability be $\Pr[X = i | S = s] = 0$ for $i \in \text{supp}(X) \setminus \text{supp}(X_s)$, in Appendix A or B, we can observe that $\sum_{i \in \text{supp}(X)} P^{x_{s_0}} = \sum_{i \in \text{supp}(X)} P^{x_{s_1}} = 1$.

The property (i) derives from the following:

$$(P^X)^{\text{tr}} V = \sum_{i \in \text{supp}(X)} P_i^X V_i = \sum_{i \in \text{supp}(X)} P_i^X \frac{P_i^{X_{s_0}} - P_i^{X_{s_1}}}{P_i^X} = \sum_{i \in \text{supp}(X)} P_i^{X_{s_0}} - P_i^{X_{s_1}} = 0.$$

The property (ii) is proved via contradiction. If $V_i > 0$ for $i \in \text{supp}(X)$, such that $P_i^{X_0} - P_i^{X_1} > 0$ for $i \in \text{supp}(X)$, hence $\sum_{i \in \text{supp}(X)} (P_i^{X_0} - P_i^{X_1}) = \sum_{i \in \text{supp}(X)} P_i^{X_0} - \sum_{i \in \text{supp}(X)} P_i^{X_1} = 1 - 1 > 0$. This contradiction shows that entries of V cannot be all positive. The contradiction for all negative is similar.

The property (iii) derives from:

$$\|V\|_1 \leq \|P^{X_{s_0}} - P^{X_{s_1}}\|_1 \left\| \frac{1}{P^X} \right\|_1 \leq (\|P^{X_{s_0}}\|_1 + \|P^{X_{s_1}}\|_1) \left\| \frac{1}{P^X} \right\|_1 = 2 \left\| \frac{1}{P^X} \right\|_1,$$

where the minus and division operators are element-wise. The first inequality uses Hölder's inequality, and the second inequality uses triangle inequality. The equality uses the fact that vectors $P^{X_{s_0}}, P^{X_{s_1}}$ are from the set Σ_N . Hence, if the norm $\left\| \frac{1}{P^X} \right\|_1$ is finite, vector V has finite l_1 norm, such that there are not infinite entries in V .

Appendix D. Proof of Lemma 10

Using TV distance in Definition 9, we can deduce that

$$\text{TV} \left(P^{\tilde{X}_{s_0}}, P^{\tilde{X}_{s_1}} \right) = \frac{1}{2} \| P^{\tilde{X}_{s_0}} - P^{\tilde{X}_{s_1}} \|_1 = \frac{1}{2} \left\| \gamma^{\text{tr}} \left(\frac{P^{X_{s_0}} - P^{X_{s_1}}}{P^X} \right) \right\|_1 = \frac{1}{2} \| \gamma^{\text{tr}} V \|_1, \quad (44)$$

where the second equation follows from Lemma 6 such that $P^{\tilde{X}_s} = \frac{P^{X_s}}{P^X}$, with the division operator being element-wise. The third equation follows from the definition of vector V in Theorem 7. Note that when $V_i = 0$, $\gamma_{i,j}, j \in \text{supp}(\tilde{X})$ could be any value without affecting the distance $\text{TV} \left(P^{\tilde{X}_{s_0}}, P^{\tilde{X}_{s_1}} \right)$, such that

$$\text{TV} \left(P^{\tilde{X}_{s_0}}, P^{\tilde{X}_{s_1}} \right) = \frac{1}{2} \sum_{j \in \text{supp}(\tilde{X})} \left| \sum_{i \in \text{supp}(X)} \gamma_{i,j} V_i \right| \quad (45)$$

$$\leq \frac{N}{2} \max_{j \in \text{supp}(\tilde{X})} \left| \sum_{i \in \text{supp}(X)} \gamma_{i,j} V_i \right| = \frac{N}{2} \max_{j \in \text{supp}(\tilde{X})} \left| \sum_{i \in \overline{\text{supp}(X)}} \gamma_{i,j} V_i \right|, \quad (46)$$

where $\overline{\text{supp}(X)} := \{i \in \text{supp}(X) \mid V_i \neq 0\}$. Given the assumption that V has finite l_1 norm, we can find a nonnegative vector Θ with entries $\Theta_j := \left| \sum_{i \in \overline{\text{supp}(X)}} \gamma_{i,j} V_i \right|$, the following holds

$$-\Theta_j \leq \sum_{i \in \overline{\text{supp}(X)}} \gamma_{i,j} V_i \leq \Theta_j, \quad \forall j \in \text{supp}(\tilde{X}), \quad (47)$$

such that the vector V is bounded by Θ , i.e., $\| \gamma^{\text{tr}} V \|_1 \leq \| \Theta \|_1$. Using Equation (44), we know that $\text{TV} \left(P^{\tilde{X}_{s_0}}, P^{\tilde{X}_{s_1}} \right) = \| \gamma^{\text{tr}} V \|_1 \leq \| \Theta \|_1$.

Appendix E. Feasibility proof of Lemma 12

The subset of all admissible couplings is

$$\Pi_{\Theta}(P^X, P^{\tilde{X}}) := \{ \gamma \in \Sigma_N^2 \mid \gamma \mathbb{1} = P^X, \gamma^{\text{tr}} \mathbb{1} = P^{\tilde{X}}, |\gamma^{\text{tr}} V|_j \leq \Theta_j, \forall j \in \text{supp}(\tilde{X}) \},$$

where $|\gamma^{\text{tr}} V|_j := \left| \sum_{i \in \text{supp}(X)} \gamma_{i,j} V_i \right|$. Recall the definition of feasible couplings in Equation (2), we can equivalently write

$$\Pi_{\Theta}(P^X, P^{\tilde{X}}) = \Pi(P^X, P^{\tilde{X}}) \cap \left\{ |\gamma^{\text{tr}} V|_j \leq \Theta_j, \forall j \in \text{supp}(\tilde{X}) \right\},$$

such that $\Pi_{\Theta}(P^X, P^{\tilde{X}}) \subseteq \Pi(P^X, P^{\tilde{X}})$. Now for any two nonnegative vectors $\Theta', \Theta \in \mathbb{R}_+^N$, with their entries satisfying $0 \leq \Theta'_j \leq \Theta_j$ for all $j \in \text{supp}(\tilde{X})$, the following holds

$$\left\{ |\gamma^{\text{tr}} V|_j \leq \Theta'_j, \forall j \in \text{supp}(\tilde{X}) \right\} \subseteq \left\{ |\gamma^{\text{tr}} V|_j \leq \Theta_j, \forall j \in \text{supp}(\tilde{X}) \right\}.$$

Hence, we can deduce that

$$\begin{aligned} \Pi(P^X, P^{\tilde{X}}) \cap \left\{ |\gamma^{\text{tr}} V|_j \leq \Theta'_j, \forall j \in \text{supp}(\tilde{X}) \right\} &\subseteq \Pi(P^X, P^{\tilde{X}}) \cap \left\{ |\gamma^{\text{tr}} V|_j \leq \Theta_j, \forall j \in \text{supp}(\tilde{X}) \right\} \\ &\iff \Pi_{\Theta'}(P^X, P^{\tilde{X}}) \subseteq \Pi_{\Theta}(P^X, P^{\tilde{X}}). \end{aligned} \quad (48)$$

The set $\Pi_{\Theta}(P^X, P^{\tilde{X}})$ becomes $\Pi(P^X, P^{\tilde{X}})$ when Θ approaches infinity, and it becomes $\Pi_0(P^X, P^{\tilde{X}})$ when Θ is zero. Along with Equation (48), we conclude the following sequence

$$\Pi_0(P^X, P^{\tilde{X}}) \subseteq \Pi_{\Theta'}(P^X, P^{\tilde{X}}) \subseteq \Pi_{\Theta}(P^X, P^{\tilde{X}}) \subseteq \Pi(P^X, P^{\tilde{X}}). \quad (49)$$

Next, we show that the set $\Pi_0(P^X, P^{\tilde{X}})$ is not empty. Remark 2.13 in Peyré et al. (2019) states that $\Pi(P^X, P^{\tilde{X}})$ is not empty with an example of $P^X \otimes P^{\tilde{X}} \in \Pi(P^X, P^{\tilde{X}})$, where \otimes is the outer product. To verify this, we define a coupling γ with its entries being $\gamma_{i,j} := P_i^X P_j^{\tilde{X}}$. Using the fact $\sum_{i \in \text{supp}(X)} P_i^X = \sum_{j \in \text{supp}(\tilde{X})} P_j^{\tilde{X}} = 1$, we observe

$$\begin{aligned} \sum_{j \in \text{supp}(\tilde{X})} \gamma_{i,j} &= \sum_{j \in \text{supp}(\tilde{X})} P_i^X P_j^{\tilde{X}} = P_i^X \sum_{j \in \text{supp}(\tilde{X})} P_j^{\tilde{X}} = P_i^X, \forall i \in \text{supp}(X); \\ \sum_{i \in \text{supp}(X)} \gamma_{i,j} &= \sum_{i \in \text{supp}(X)} P_i^X P_j^{\tilde{X}} = P_j^{\tilde{X}} \sum_{i \in \text{supp}(X)} P_i^X = P_j^{\tilde{X}}, \forall j \in \text{supp}(\tilde{X}); \end{aligned}$$

such that this coupling does belong to $\Pi(P^X, P^{\tilde{X}})$. Using Property (i) in Remark 8, we further observe

$$\sum_{i \in \text{supp}(X)} \gamma_{i,j} V_i = P_j^{\tilde{X}} \sum_{i \in \text{supp}(X)} P_i^X V_i = P_j^{\tilde{X}} \times ((P^X)^{\text{tr}} V) = 0, \forall j \in \text{supp}(\tilde{X}),$$

such that this coupling also belongs to $\Pi_0(P^X, P^{\tilde{X}})$. Since we found one coupling in the set $\Pi_0(P^X, P^{\tilde{X}})$, this set is not empty. Using Equation (49), we know that for arbitrary nonnegative $\Theta \in \mathbb{R}_+^N$, the feasible set of our formulation in Equation (22) is not empty, i.e., $\Pi_{\Theta}(P^X, P^{\tilde{X}}) \neq \emptyset$, such that the solutions of our formulation exist.

Appendix F. Proof of Lemma 13

The proof uses subgradient optimality conditions that can be found in Proposition 5.4.7 in Bertsekas (2009). We start from restating the constrained KL projection as an unconstrained problem:

$$\mathcal{P}_{\mathcal{C}}^{KL}(\bar{\gamma}) = \arg \min_{\gamma \in \mathcal{C}} \text{KL}(\gamma \| \bar{\gamma}) = \arg \min_{\gamma \in \mathbb{R}_+^{N \times N}} \text{KL}(\gamma \| \bar{\gamma}) + \iota_{\mathcal{C}}(\gamma). \quad (50)$$

The indicator function of a convex set \mathcal{C} is a convex function, see Section 2 in Ekeland and Temam (1999). Further, $\iota_{\mathcal{C}}$ is lower semi-continuous if and only if \mathcal{C} is closed. Since \mathcal{C} is a closed convex set (e.g., affine hyperplanes, closed half-spaces bounded by affine hyperplanes), $\iota_{\mathcal{C}}$ is a convex, lower semi-continuous coercive function. Also, $\text{KL}(\cdot \| \bar{\gamma})$ is a strictly convex and coercive function. This operator is uniquely defined by strict convexity.

As $\text{KL}(\cdot\|\bar{\gamma})$ is a Gateaux differential function with derivative $\nabla \text{KL}(\gamma\|\bar{\gamma}) = \partial \text{KL}(\gamma\|\bar{\gamma}) = \log(\gamma/\bar{\gamma})$. Then the necessary and sufficient condition for γ^* being the minimiser is

$$\mathbf{0} \in \partial(\text{KL}(\gamma^*\|\bar{\gamma}) + \iota_{\mathcal{C}}(\gamma^*)) = \log\left(\frac{\gamma^*}{\bar{\gamma}}\right) + \partial\iota_{\mathcal{C}}(\gamma^*), \quad (51)$$

where $\partial\iota_{\mathcal{C}}(\gamma^*)$ is the set of all subgradients at γ^* , and $\mathbf{0}$ is an $N \times N$ zero matrix. The equation comes from $\text{dom KL}(\cdot\|\bar{\gamma}) \cap \text{dom } \iota_{\mathcal{C}} \neq \emptyset$ and Moreau-Rockafellar theorem. To prove this optimality condition, define a function $J(\gamma) = \text{KL}(\gamma\|\bar{\gamma}) + \iota_{\mathcal{C}}(\gamma)$ on $\mathbb{R}_+^{N \times N}$. Due to $J(\gamma) \geq J(\gamma^*)$ for all $\gamma \in \mathbb{R}_+^{N \times N}$, if $\mathbf{0} \in \partial J(\gamma^*)$, then the definition of subgradients in Equation (29) implies $J(\gamma) \geq J(\gamma^*) + \langle \mathbf{0}, (\gamma - \gamma^*) \rangle$ for all $\gamma \in \mathbb{R}_+^{N \times N}$.

Appendix G. Proof of Lemma 14

The proof is based on Peyré (2015) and Benamou et al. (2015).

Let $\gamma^* = \mathcal{P}_{\mathcal{C}_\ell}^{KL}(\bar{\gamma})$. For the first case, i.e., $\ell = 1$, note that

$$\iota_{\mathcal{C}_1}(\gamma) = \iota_{P^X}(\gamma\mathbf{1}). \quad (52)$$

Let $u \in \partial\iota_{P^X}(P^*) \subset \mathbb{R}^N$, where $P^* = \gamma^*\mathbf{1}$. According to Lemma 13, the following holds

$$\mathbf{0} = \log\left(\frac{\gamma^*}{\bar{\gamma}}\right) + u\mathbf{1}^{\text{tr}} \Rightarrow \gamma^* = \text{diag}(\exp(-u))\bar{\gamma}. \quad (53)$$

Plug in $\gamma^*\mathbf{1} = P^X$,

$$\gamma^*\mathbf{1} = \text{diag}(\exp(-u))\bar{\gamma}\mathbf{1} = P^X \Rightarrow \gamma^* = \text{diag}\left(\frac{P^X}{\bar{\gamma}\mathbf{1}}\right)\bar{\gamma}. \quad (54)$$

For the second case, i.e., $\ell = 2$, the optimality condition becomes

$$\mathbf{0} = \log\left(\frac{\gamma^*}{\bar{\gamma}}\right) + \mathbf{1}\nu^{\text{tr}} \Rightarrow \gamma^* = \bar{\gamma} \text{diag}(\exp(-\nu)), \quad (55)$$

where $\nu \in \partial\iota_{P^{\tilde{X}}}((\gamma^*)^{\text{tr}}\mathbf{1}) \subset \mathbb{R}^N$. Using $(\gamma^*)^{\text{tr}}\mathbf{1} = P^{\tilde{X}}$,

$$(\gamma^*)^{\text{tr}}\mathbf{1} = \text{diag}(\exp(-\nu))\bar{\gamma}^{\text{tr}}\mathbf{1} = P^{\tilde{X}} \Rightarrow \gamma^* = \bar{\gamma} \text{diag}\left(\frac{P^{\tilde{X}}}{\bar{\gamma}^{\text{tr}}\mathbf{1}}\right). \quad (56)$$

Appendix H. Proof of Lemma 15

Let $\gamma^* = \mathcal{P}_{\mathcal{C}_3}^{KL}(\bar{\gamma})$. First notice that if some parts of $\bar{\gamma}$ already satisfy the constraint in \mathcal{C}_3 , these parts should carry over to γ^* in order to minimise the term $\text{KL}(\gamma^*\|\bar{\gamma})$ in the objective function of $\mathcal{P}_{\mathcal{C}_3}^{KL}$. If $\bar{\gamma} \in \mathcal{C}_3$, it is straightforward $\gamma^* = \bar{\gamma}$. Further, since \mathcal{C}_3 has not relevance to these entries $i \notin \overline{\text{supp}(X)}$, $j \in \text{supp}(\tilde{X})$ of $\bar{\gamma}$, we know that $\gamma_{i,j}^* = \bar{\gamma}_{i,j}$, for $i \notin \overline{\text{supp}(X)}$, $j \in \text{supp}(\tilde{X})$. Also, if the constraint $-\Theta_j \leq \sum_{i \in \overline{\text{supp}(X)}} \bar{\gamma}_{i,j} V_i \leq \Theta_j$ is satisfied for certain $j^\dagger \in \text{supp}(\tilde{X})$, we should set these entries $\gamma_{i,j}^* = \bar{\gamma}_{i,j}$, for all qualified j^\dagger and $i \in \text{supp}(X)$.

Therefore, we only discuss the case that $\bar{\gamma} \notin \mathcal{C}_3$ and the entries (i, j) that $i \in \overline{\text{supp}(\tilde{X})}$ and $j \in \{\text{supp}(\tilde{X}) \mid [\bar{\gamma}^{\text{tr}}V]_j \notin [-\Theta_j, \Theta_j]\}$.

According to Lemma 13, the optimality condition becomes

$$\mathbb{0} = \log\left(\frac{\gamma^*}{\bar{\gamma}}\right) + V\nu^{\text{tr}} \Rightarrow \gamma^* = \bar{\gamma} \odot \exp(-V\nu^{\text{tr}}), \quad (57)$$

where \odot is element-wise product and $\nu \in \partial\iota_{\Theta}(P^*) \subset \mathbb{R}^N$, $P^* = (\gamma^*)^{\text{tr}}V$. The indicator function $\iota_{\Theta}(P)$ is 0 if $-\Theta \leq P \leq \Theta$ and infinity otherwise. Recall the definition of subgradient in Lemma 13. The following holds

$$\langle \nu, (\gamma - \gamma^*)^{\text{tr}}V \rangle + \iota_{\Theta}((\gamma^*)^{\text{tr}}V) \leq \iota_{\Theta}(\gamma^{\text{tr}}V), \forall \gamma \in \mathbb{R}_+^{N \times N}. \quad (58)$$

Now, we discuss the conditions imposed on existence of (at least) one subgradient, such that the subdifferential $\partial\iota_{\Theta}(P^*) \neq \emptyset$, where $P^* = (\gamma^*)^{\text{tr}}V$. If $\gamma^* \notin \mathcal{C}_3$, $\iota_{\Theta}((\gamma^*)^{\text{tr}}V) = +\infty$, there is not such ν can satisfy Equation (58). Hence, we must have $\gamma^* \in \mathcal{C}_3$ to ensure the existence of (at least) one subgradient ν . Further, the right part of Equation (58) is $\iota_{\Theta}(\gamma^{\text{tr}}V) = 0$ if the arbitrary matrix $\gamma \in \mathcal{C}_3$, and $\iota_{\Theta}(\gamma^{\text{tr}}V) = \infty$ if the arbitrary matrix $\gamma \notin \mathcal{C}_3$, while this inequality in Equation (58) holds for any arbitrary matrix γ . We equivalently simplify the condition in Equation (58) into for all $\gamma \in \mathcal{C}_3$, the following holds

$$\langle \nu, (\gamma - \gamma^*)^{\text{tr}}V \rangle \leq 0 \Rightarrow \nu^{\text{tr}}\gamma^{\text{tr}}V \leq \nu^{\text{tr}}(\gamma^*)^{\text{tr}}V.$$

Now, we gather these conditions found so far:

$$\boxed{\nu^{\text{tr}}\gamma^{\text{tr}}V \leq \nu^{\text{tr}}(\gamma^*)^{\text{tr}}V, \forall \gamma \in \mathcal{C}_3; \quad \gamma^* = \bar{\gamma} \odot \exp(-V\nu^{\text{tr}}); \quad \gamma^* \in \mathcal{C}_3.} \quad (59)$$

- If $\Theta = \mathbb{0}$, given the third condition in Equation (59), the first condition holds for any $\nu \in \mathbb{R}$ because $\gamma^{\text{tr}}V = (\gamma^*)^{\text{tr}}V = \mathbb{0}$. The last two conditions require that ν needs to satisfy

$$(\gamma^*)^{\text{tr}}V = [\bar{\gamma} \odot \exp(-V\nu^{\text{tr}})]^{\text{tr}}V = \mathbb{0}.$$

- If $\Theta \neq \mathbb{0}$, to make sure there exists (at least) one subgradient ν that satisfies the first condition $\nu^{\text{tr}}\gamma^{\text{tr}}V \leq \nu^{\text{tr}}(\gamma^*)^{\text{tr}}V$, for any arbitrary matrix $\gamma \in \mathcal{C}_3$, the optimal solution γ^* must be on the edge of \mathcal{C}_3 :

$$[(\gamma^*)^{\text{tr}}V]_j = \Theta_j \text{ or } -\Theta_j, \forall j \in \text{supp}(\tilde{X}). \quad (60)$$

It is obvious that the sign of ν_j should be the same as the sign of $[(\gamma^*)^{\text{tr}}V]_j$.

Recall that we only focus on the cases that $\bar{\gamma} \notin \mathcal{C}_3$. Hence, there are some $j \in \text{supp}(\tilde{X})$:

$$\sum_{i,j=1}^N \bar{\gamma}_{i,j} V_i > \Theta_j \text{ or } \sum_{i,j=1}^N \bar{\gamma}_{i,j} V_i < -\Theta_j.$$

As the exponential function is positive, i.e., $\exp(-V_i\nu_j) > 0$, we cannot change the sign of $[(\gamma^*)^{\text{tr}}V]_j$ by adjusting ν . Hence, the last two conditions in Equation (59) imply that the subgradient ν should satisfy

$$[(\gamma^*)^{\text{tr}}V]_j = \sum_{i,j=1}^N \bar{\gamma}_{i,j} \exp(-V_i\nu_j) V_i = \begin{cases} \Theta_j & \text{if } \sum_{i,j=1}^N \bar{\gamma}_{i,j} V_i > \Theta_j \\ -\Theta_j & \text{if } \sum_{i,j=1}^N \bar{\gamma}_{i,j} V_i < -\Theta_j \end{cases}, \forall j \in \text{supp}(\tilde{X}). \quad (61)$$

Once the subgradient ν is found, plug in the second condition in Equation (59), we find the optimal solution γ^* .

Please be aware that the first and third conditions in Equation (59) guarantees the existence of subgradient ν , i.e., the subdifferential is not empty, while we also need (at least) one ν in the subdifferential to satisfy the second condition (i.e., the optimality condition). The existence of such subgradient ν that satisfies Equation (60) or (61) is discussed in Appendix I.

Appendix I. Existence proof of Remark 16

Recall the definition of ν_j in the case of $\Theta \neq \mathbf{0}$ in Equation (61), with the case of $\Theta = \mathbf{0}$ being a special case. Existence of such ν_j is equivalent to existence of (at least) one root of the function $F(x) := \sum_{i \in \overline{\text{supp}(X)}} \bar{\gamma}_{i,j} V_i \exp(-V_i x) + c$, where the constant $c = \pm \Theta_j$. Regardless of the values of the constant c , the first derivative of this function is $\nabla F(x) = -\sum_{i \in \overline{\text{supp}(X)}} \bar{\gamma}_{i,j} (V_i)^2 \exp(-V_i x) \leq 0$, such that $F(x)$ is non-increasing.

Now, we discuss the conditions for existence of roots (i.e., ν_j). We assume that the vector $V \neq \mathbf{0}$, because no coupling is needed if $V = \mathbf{0}$, i.e., group parity is already achieved. Assumption 1 ensures that the vector V has finite l_1 -norm, such that none of its entries are infinity. We only discuss these $j \in \text{supp}(\tilde{X})$ where $[\bar{\gamma}^{\text{tr}} V]_j > \Theta_j$ or $[\bar{\gamma}^{\text{tr}} V]_j < -\Theta_j$, because we do not need to compute ν_j for other j where $-\Theta \leq [\bar{\gamma}^{\text{tr}} V]_j \leq \Theta_j$, as mentioned in Appendix H.

- If $[\bar{\gamma}^{\text{tr}} V]_j > \Theta_j$, let $F(x) := \sum_{i \in \overline{\text{supp}(X)}} \bar{\gamma}_{i,j} V_i \exp(-V_i x) - \Theta_j$, such that ν_j is the root of $F(x)$. We first observe that

$$[\bar{\gamma}^{\text{tr}} V]_j > \Theta_j \Rightarrow F(0) = \sum_{i \in \overline{\text{supp}(X)}} \bar{\gamma}_{i,j} V_i > \Theta_j \geq 0.$$

Since $F(x)$ is non-increasing, the root of $F(x)$ must be positive if the root exists. Note that $F(x)$ is the sum of the term $\bar{\gamma}_{i,j} V_i \exp(-V_i x)$. Let $x \rightarrow +\infty$, we observe the following

$$\lim_{x \rightarrow +\infty} \bar{\gamma}_{i,j} V_i \exp(-V_i x) = \begin{cases} 0 & \text{if } V_i > 0 \text{ or } \bar{\gamma}_{i,j} = 0, \\ -\infty & \text{if } V_i < 0 \text{ and } \bar{\gamma}_{i,j} > 0. \end{cases}$$

Hence, if there exists one summand that goes to $-\infty$, the function $F(x)$ goes to $-\infty$. In other words, for a given $j \in \text{supp}(\tilde{X})$ and $[\bar{\gamma}^{\text{tr}} V]_j > \Theta_j$, as long as there exist (at least) one entry $i \in \text{supp}(X)$ satisfying both $V_i < 0$ and $\bar{\gamma}_{i,j} > 0$, we can conclude that

$$\lim_{x \rightarrow +\infty} F(x) = \lim_{x \rightarrow +\infty} \sum_{i \in \overline{\text{supp}(X)}} \bar{\gamma}_{i,j} V_i \exp(-V_i x) = -\infty.$$

Then using the fact that $F(0) > 0$ and $\lim_{x \rightarrow +\infty} F(x) = -\infty$, the root of function $F(x)$ must exist, such that ν_j exists.

- If $[\bar{\gamma}^{\text{tr}}V]_j < -\Theta_j$, let $F(x) := \sum_{i \in \overline{\text{supp}(X)}} \bar{\gamma}_{i,j} V_i \exp(-V_i x) + \Theta_j$, such that ν_j is the root. Similarly, we observe that

$$[\bar{\gamma}^{\text{tr}}V]_j < -\Theta_j \Rightarrow F(0) = \sum_{i \in \overline{\text{supp}(X)}} \bar{\gamma}_{i,j} V_i < -\Theta_j \leq 0.$$

As $F(x)$ is non-increasing, the root of $F(x)$ is negative if it exists. Let $x \rightarrow -\infty$, the summand of the function $F(x)$ goes to

$$\lim_{x \rightarrow -\infty} \bar{\gamma}_{i,j} V_i \exp(-V_i x) = \begin{cases} +\infty & \text{if } V_i > 0 \text{ and } \bar{\gamma}_{i,j} > 0, \\ 0 & \text{if } V_i < 0 \text{ or } \bar{\gamma}_{i,j} = 0. \end{cases}$$

Hence, if there exists one summand that goes to $+\infty$, the function $F(x)$ goes to $+\infty$. In other words, for a given $j \in \text{supp}(\tilde{X})$ that $[\bar{\gamma}^{\text{tr}}V]_j < -\Theta_j$, as long as there exists (at least) one entry $i \in \text{supp}(X)$ satisfying both $V_i > 0$ and $\bar{\gamma}_{i,j} > 0$, we can conclude that

$$\lim_{x \rightarrow -\infty} F(x) = \lim_{x \rightarrow +\infty} \sum_{i \in \overline{\text{supp}(X)}} \bar{\gamma}_{i,j} V_i \exp(-V_i x) = +\infty.$$

Then using the fact that $F(0) < 0$, and $\lim_{x \rightarrow -\infty} F(x) = +\infty$, the root of function $F(x)$ must exist, such that ν_j exists.

Since it always holds $\bar{\gamma}_{i,j} \geq 0$, we can conclude a sufficient condition for existence of the root for both cases. For any $j \in \text{supp}(\tilde{X})$, there exists (at least) one non-zero entry $\bar{\gamma}_{i,j}$ when $V_i < 0$ and (at least) one non-zero entry $\bar{\gamma}_{i,j}$ when $V_i > 0$.

According to Remark 8 (ii), unless $V = \mathbf{0}$, the vector V always has a mixture of positive entries and negative entries. Then, the entropic regularisation term in our formulation in Equation (22), generally promotes non-zero entries in $\bar{\gamma}$, and the entries of the initial coupling ξ are all positive. Hence, violation of this sufficient condition is almost impossible, thus ν_j exists almost surely.

The existence of ν_j only guarantees that our computation in Appendix H can find the solution of $\mathcal{P}_{\mathcal{C}_3}^{KL}(\bar{\gamma})$ as long as the root-finding algorithm converges to the root.

Appendix J. Convergence proof of Dykstra's algorithm

This section heavily depends on Bauschke and Lewis (2000) and Section 30.2 in Bauschke et al. (2017).

Assume E is some Euclidean space with inner product $\langle \cdot, \cdot \rangle$ and induced norm $\| \cdot \|$. Without loss of generality, we assume there are two closed convex sets $\mathcal{C}_1, \mathcal{C}_2$ in E with $\mathcal{C} := \mathcal{C}_1 \cap \mathcal{C}_2 \neq \emptyset$. Note that the assumption of $\mathcal{C} \neq \emptyset$ in Dykstra's algorithm is satisfied due to our feasibility results in Lemma 12.

Definition 22 (Bregman projections) *The general Bregman projection of ξ onto \mathcal{C} respect to a Legendre function φ on E and the corresponding Bregman distance*

$$D_\varphi : E \times \text{int}(\text{dom } \varphi) \rightarrow [0, +\infty] : \\ (\gamma, \xi) \mapsto \varphi(\gamma) - \varphi(\xi) - \langle \nabla \varphi(\xi), \gamma - \xi \rangle,$$

is to solve the optimisation problem:

$$\mathcal{P}_{\mathcal{C}}^{\varphi}(\xi) := \min_{\gamma \in \mathcal{C} \cap \text{dom } \varphi} D_{\varphi}(\gamma, \xi).$$

Note that when $\varphi(\gamma) := \sum_{i,j} \gamma_{i,j} \log \gamma_{i,j}$, the general Bregman divergence is KL divergence, as defined in Equation (4).

Given an arbitrary point ξ in E . Since only the KL projection is considered in this paper, we use $\mathcal{P}_{\mathcal{C}}(\xi)$ in place of $\mathcal{P}_{\mathcal{C}}^{\varphi}(\xi)$, to denote the point in \mathcal{C} that is the nearest to ξ , and we assume $\mathcal{C}_k := \mathcal{C}_k \cap \text{int}(\text{dom } \varphi)$, $k = 1, 2$ for ease of notation. The Dykstra's algorithm in Boyle and Dykstra (1986); Bauschke et al. (2017) sets $\gamma_0 := \xi, q_0 = q_{-1} = q_{-2} := 0$, and then iteratively conducts the following sequences for $k \geq 1$:

$$\gamma_k := \mathcal{P}_{\mathcal{C}_k}(\gamma_{k-1} + q_{k-2}), \quad q_k := \gamma_{k-1} + q_{k-2} - \gamma_k, \quad (62)$$

where the “2” comes from the number of convex sets considered in this problem, and $\mathcal{P}_{\mathcal{C}_k}$ is the Bregman projections onto the convex set $\mathcal{C}_{(k \bmod 2)}$. The sequence $\{\gamma_k\}_{k \geq 1}$ converges strongly to $\mathcal{P}_{\mathcal{C}}(\xi)$, Boyle and Dykstra (1986).

Lemma 23 (Theorem 3.16 in Bauschke et al. (2017)) *When \mathcal{C} is a nonempty closed convex subset of E , for every $x, \gamma_k \in E$,*

$$\gamma_k = \mathcal{P}_{\mathcal{C}}(x) \Leftrightarrow \gamma_k \in \mathcal{C} \text{ and } \langle c - \gamma_k, x - \gamma_k \rangle \leq 0, \forall c \in \mathcal{C}.$$

Lemma 24 *For any $k > 0$, $\gamma_k = \mathcal{P}_{\mathcal{C}_k}(\gamma_{k-1} + q_{k-2})$ and then for any $c \in \mathcal{C}_k$, the following holds*

$$\gamma_k \in \mathcal{C}_k, \quad \langle c - \gamma_k, q_k \rangle \leq 0.$$

Proof *From Lemma 23 and Equation (62), as \mathcal{C}_k is a nonempty closed convex subset of E , we deduce that for $(\gamma_{k-1} + q_{k-2}), \gamma_k \in E$, the following holds*

$$\gamma_k = \mathcal{P}_{\mathcal{C}_k}(\gamma_{k-1} + q_{k-2}) \Leftrightarrow \gamma_k \in \mathcal{C}_k \text{ and } \langle c - \gamma_k, \gamma_{k-1} + q_{k-2} - \gamma_k \rangle = \langle c - \gamma_k, q_k \rangle \leq 0. \quad \blacksquare$$

Lemma 25 *The sequence $\{\gamma_k\}_{k \geq 1}$ is bounded and $\gamma_{k-1} - \gamma_k \rightarrow 0$, where the arrow “ \rightarrow ” refers to strong convergence.*

Proof *From Equation (62), for any $k \geq 1$, the following holds*

$$\gamma_{k-1} - \gamma_k = q_k - q_{k-2}. \quad (63)$$

Let $c \in \mathcal{C}$, we deduce that

$$\begin{aligned} \|\gamma_k - c\|^2 &= \|\gamma_{k+1} - c\|^2 + \|\gamma_k - \gamma_{k+1}\|^2 + 2\langle \gamma_{k+1} - c, \gamma_k - \gamma_{k+1} \rangle \\ &= \|\gamma_{k+1} - c\|^2 + \|\gamma_k - \gamma_{k+1}\|^2 + 2\langle \gamma_{k+1} - c, q_{k+1} - q_{k-1} \rangle, \end{aligned}$$

where the second equality used Equation (63). Then we rewrite the equation above into

$$\|\gamma_{k+1}-c\|^2-\|\gamma_k-c\|^2=-\|\gamma_k-\gamma_{k+1}\|^2-2\langle\gamma_{k+1}-c,q_{k+1}\rangle-2\langle\gamma_{k-1}-\gamma_{k+1},q_{k-1}\rangle+2\langle\gamma_{k-1}-c,q_{k-1}\rangle.$$

Using induction, we deduce that for $l \geq n$, the following holds

$$\begin{aligned} & \|\gamma_l-c\|^2-\|\gamma_n-c\|^2 \\ &= \sum_{k=n}^{l-1} \left(\|\gamma_{k+1}-c\|^2-\|\gamma_k-c\|^2 \right) \\ &= -\sum_{k=n}^{l-1} \left(\|\gamma_k-\gamma_{k+1}\|^2+2\langle\gamma_{k-1}-\gamma_{k+1},q_{k-1}\rangle \right) + \sum_{k=n}^{l-1} \left(2\langle\gamma_{k-1}-c,q_{k-1}\rangle-2\langle\gamma_{k+1}-c,q_{k+1}\rangle \right) \\ &= -\sum_{k=n}^{l-1} \left(\|\gamma_k-\gamma_{k+1}\|^2+2\langle\gamma_{k-1}-\gamma_{k+1},q_{k-1}\rangle \right) + 2\sum_{k=n-1}^n \langle\gamma_{k-1}-c,q_{k-1}\rangle - 2\sum_{k=l}^{l+1} \langle\gamma_{k+1}-c,q_{k+1}\rangle. \end{aligned}$$

Now, set $n=0$, such that $2\sum_{k=n-1}^n \langle\gamma_{k-1}-c,q_{k-1}\rangle=0$ by $q_{-1}=q_{-2}=0$. We have

$$\|\gamma_l-c\|^2-\|\xi-c\|^2=-\sum_{k=0}^{l-1} \left(\|\gamma_k-\gamma_{k+1}\|^2+2\langle\gamma_{k-1}-\gamma_{k+1},q_{k-1}\rangle \right) - 2\sum_{k=l}^{l+1} \langle\gamma_{k+1}-c,q_{k+1}\rangle. \quad (64)$$

By definition in Equation (62), $\gamma_{k-1}, \gamma_{k+1}, c \in \mathcal{C}_{(k-1 \bmod 2)}$. Using Lemma 24, we have

$$\langle\gamma_{k-1}-\gamma_{k+1},q_{k-1}\rangle \geq 0, \langle\gamma_{k+1}-c,q_{k+1}\rangle \geq 0.$$

Go back to Equation (64), we can deduce that

$$\|\gamma_l-c\|^2 \leq \|\xi-c\|^2, \forall l \geq 1,$$

such that the sequence $\{\gamma_k\}_{k \geq 1}$ is bounded and $\lim_l \sum_{k=0}^{l-1} \|\gamma_k-\gamma_{k+1}\|^2 < +\infty$. We can now conclude that the sequence of partial sums $\{\sum_{k=0}^{l-1} \|\gamma_k-\gamma_{k+1}\|^2\}_{l \geq 1}$ is a monotone nonnegative real sequence with bounded limit, then the difference $\gamma_k-\gamma_{k+1}$ tend to zero. \blacksquare

Lemma 26 (Lemma 30.6 in Bauschke et al. (2017)) Suppose $\{p_k\}_{k \geq 1}$ is a sequence of nonnegative reals with $\sum_k p_k^2 < +\infty$. Let $\sigma_n := \sum_{k=1}^n p_k$. Then $\liminf_n \sigma_n(\sigma_n - \sigma_{n-m-1}) = 0$, for an arbitrary $1 \leq m \leq n$.

Lemma 27

$$\liminf_n |\langle\gamma_{n-1}-\gamma_n,q_k\rangle| = 0.$$

Proof Since $q_k = (q_k - q_{k-2}) + (q_{k-2} - q_{k-4}) + \dots + (q_{(k \bmod 2)} - q_{(k \bmod 2)-2})$, using triangle inequality for norm, we have

$$\|q_{n-1}\| \leq \|q_n\| + \|q_{n-1}\| \leq \sum_{k=1}^n \|q_k - q_{k-2}\| = \sum_{k=1}^n \|\gamma_{k-1} - \gamma_k\|, \quad (65)$$

where the equality utilises Equation (63). The case of $k = 0$ is omitted because q_0, q_{-1}, q_{-2} are zero. Further,

$$\begin{aligned} |\langle \gamma_{n-1} - \gamma_n, q_{n-1} \rangle| &\leq \|\gamma_{n-1} - \gamma_n\| \|q_{n-1}\| \\ &\leq \|\gamma_{n-1} - \gamma_n\| \left(\sum_{k=1}^n \|\gamma_{k-1} - \gamma_k\| \right). \end{aligned}$$

The first inequality uses Cauchy-Schwarz inequality. The second one uses Equation (65). Then, using Lemma 25 and 26, we complete the proof. \blacksquare

Lemma 28 For any $c \in \mathcal{C}$,

$$\langle c - \gamma_n, \xi - \gamma_n \rangle = \sum_{k=n-1}^n \langle c - \gamma_k, q_k \rangle + \sum_{k=n-1}^n \langle \gamma_k - \gamma_n, q_k \rangle$$

Proof Applying induction to Equation (63), we observe that

$$\xi - \gamma_n = \sum_{k=1}^n \gamma_{k-1} - \gamma_k = \sum_{k=1}^n q_k - q_{k-2} = \sum_{k=n-1}^n q_k. \quad (66)$$

Hence,

$$\langle c - \gamma_n, \xi - \gamma_n \rangle = \sum_{k=n-1}^n \langle c - \gamma_n, q_k \rangle = \sum_{k=n-1}^n \langle c - \gamma_k, q_k \rangle + \sum_{k=n-1}^n \langle \gamma_k - \gamma_n, q_k \rangle.$$

\blacksquare

Lemma 29 (Lemma 2.42 in Bauschke et al. (2017)) If γ_{k_n} converges weakly to $c^* \in \mathcal{C}$, then

$$\|c^*\| \leq \liminf_n \|\gamma_{k_n}\|.$$

Proof By Cauchy-Schwarz inequality,

$$\|c^*\|^2 = \lim_n |\langle \gamma_{k_n}, c^* \rangle| \leq \liminf_n \|\gamma_{k_n}\| \|c^*\|.$$

\blacksquare

Theorem 30 (Boyle and Dykstra (1986)) We can find a subsequence $\{k_n\}_{n \geq 1}$ of $\{k\}_{k \geq 1}$ with

$$\lim_n |\langle \gamma_{k_n-1} - \gamma_{k_n}, q_k \rangle| = 0. \quad (67)$$

This subsequence converges weakly to $P_{\mathcal{C}}(\xi) \in \mathcal{C}$.

Proof From the definition of the subsequence, $\{\gamma_{k_n}\}_{n \geq 1}$ converges weakly to some $c^* \in \text{int}(\text{dom } \varphi)$ and $\lim_n \|\gamma_{k_n}\|$ exists. From the definition of the sequence in Equation 62, we know that $\gamma_{k_n} \in \mathcal{C}_{(k_n \bmod 2)}$ for $k_n > 0$. Using Lemma 25, we know that $c^* \in \mathcal{C}$.

Further, we can deduce from Lemma 24 and 28 that for any $c \in \mathcal{C}$:

$$\begin{aligned} \limsup_n \langle c - \gamma_{k_n}, \xi - \gamma_{k_n} \rangle &= \limsup_n \left(\sum_{l=k_n-1}^{k_n} \langle c - \gamma_l, q_l \rangle + \sum_{l=k_n-1}^{k_n} \langle \gamma_l - \gamma_{k_n}, q_l \rangle \right) \\ &= \limsup_n \sum_{l=k_n-1}^{k_n} \langle c - \gamma_l, q_l \rangle \leq 0. \end{aligned}$$

Lemma 29 shows that if γ_{k_n} converges weakly to c^* , for any $c \in \mathcal{C}$,

$$\langle c - c^*, \xi - c^* \rangle \leq \limsup_n \langle c - \gamma_{k_n}, \xi - \gamma_{k_n} \rangle \leq 0. \quad (68)$$

Combining Equation (68) and Lemma 23, we conclude that $c^* = P_{\mathcal{C}}(\xi)$, such that this subsequence converges weakly to $P_{\mathcal{C}}(\xi)$. \blacksquare

For the case of two convex sets $\mathcal{C}_1, \mathcal{C}_2$, the fact that the subsequence converges weakly to $P_{\mathcal{C}}(\xi)$ and $\lim_n \|\gamma_n - \gamma_{n+1}\| = 0$ by Lemma 25 are sufficient to show that the whole sequence converges strongly to $P_{\mathcal{C}}(\xi)$. For the strong convergence proof of more than two convex sets, we refer to Section 30.2 in Bauschke et al. (2017) and Bauschke and Lewis (2000) for more details.

References

- Martial Agueh and Guillaume Carlier. Barycenters in the Wasserstein space. *SIAM Journal on Mathematical Analysis*, 43(2):904–924, 2011.
- Hilary J Allen. Regulatory sandboxes. *Geo. Wash. L. Rev.*, 87:579, 2019.
- Alexander Amini, Ava P Soleimany, Wilko Schwarting, Sangeeta N Bhatia, and Daniela Rus. Uncovering and mitigating algorithmic bias through learned latent structure. In *Proceedings of the 2019 AAAI/ACM Conference on AI, Ethics, and Society*, pages 289–295, 2019.
- McKane Andrus and Sarah Villeneuve. Demographic-reliant algorithmic fairness: Characterizing the risks of demographic data collection in the pursuit of fairness. In *Proceedings of the 2022 ACM Conference on Fairness, Accountability, and Transparency, FAccT ’22*, page 1709–1721, New York, NY, USA, 2022. Association for Computing Machinery. ISBN 9781450393522. doi: 10.1145/3531146.3533226. URL <https://doi.org/10.1145/3531146.3533226>.
- Julia Angwin, Jeff Larson, Surya Mattu, and Lauren Kirchner. Machine bias. In *Ethics of data and analytics*, pages 254–264. Auerbach Publications, 2022.

- Solon Barocas, Moritz Hardt, and Arvind Narayanan. *Fairness and Machine Learning: Limitations and Opportunities*. fairmlbook.org, 2019. <http://www.fairmlbook.org>.
- Heinz H Bauschke and Adrian S Lewis. Dykstras algorithm with Bregman projections: A convergence proof. *Optimization*, 48(4):409–427, 2000.
- Heinz H Bauschke, Patrick L Combettes, Heinz H Bauschke, and Patrick L Combettes. *Correction to: Convex Analysis and Monotone Operator Theory in Hilbert Spaces*. Springer, 2017.
- Heinz H Bauschke, Regina S Burachik, Daniel B Herman, and C Yalçın Kaya. On Dykstra’s algorithm: finite convergence, stalling, and the method of alternating projections. *Optimization Letters*, 14:1975–1987, 2020.
- Yahav Bechavod and Aaron Roth. Individually fair learning with one-sided feedback. In *International Conference on Machine Learning*, pages 1954–1977. PMLR, 2023.
- Barry Becker and Ronny Kohavi. Adult. UCI Machine Learning Repository, 1996. DOI: <https://doi.org/10.24432/C5XW20>.
- Jean-David Benamou, Guillaume Carlier, Marco Cuturi, Luca Nenna, and Gabriel Peyré. Iterative Bregman projections for regularized transportation problems. *SIAM Journal on Scientific Computing*, 37(2):A1111–A1138, 2015.
- Dimitri Bertsekas. *Convex optimization theory*, volume 1. Athena Scientific, 2009.
- Reuben Binns. On the apparent conflict between individual and group fairness. In *Proceedings of the 2020 conference on fairness, accountability, and transparency*, pages 514–524, 2020.
- Emily Black, Samuel Yeom, and Matt Fredrikson. Fliptest: fairness testing via optimal transport. In *Proceedings of the 2020 Conference on Fairness, Accountability, and Transparency*, pages 111–121, 2020.
- Prasenjit Bose, Soumyadeep Biswas, and Samiran Sengupta. The case for caste census in india — explained. *The Hindu*, October 12th, 2023. URL <https://www.thehindu.com/news/national/explained-the-case-for-caste-census-in-india/article67411718.ece>.
- James P Boyle and Richard L Dykstra. A method for finding projections onto the intersection of convex sets in Hilbert spaces. In *Advances in Order Restricted Statistical Inference: Proceedings of the Symposium on Order Restricted Statistical Inference held in Iowa City, Iowa, September 11–13, 1985*, pages 28–47. Springer, 1986.
- Lev M Bregman. The relaxation method of finding the common point of convex sets and its application to the solution of problems in convex programming. *USSR computational mathematics and mathematical physics*, 7(3):200–217, 1967.
- Maarten Buyl and Tijl De Bie. Optimal transport of classifiers to fairness. *Advances in Neural Information Processing Systems*, 35:33728–33740, 2022.

- Luis A Caffarelli and Robert J McCann. Free boundaries in optimal transport and Monge-Ampere obstacle problems. *Annals of mathematics*, pages 673–730, 2010.
- Toon Calders and Indrė Žliobaitė. Why unbiased computational processes can lead to discriminative decision procedures. In *Discrimination and Privacy in the Information Society: Data mining and profiling in large databases*, pages 43–57. Springer, 2013.
- Flavio Calmon, Dennis Wei, Bhanukiran Vinzamuri, Karthikeyan Natesan Ramamurthy, and Kush R Varshney. Optimized pre-processing for discrimination prevention. *Advances in neural information processing systems*, 30, 2017.
- Alessandro Castelnovo, Riccardo Crupi, Greta Greco, Daniele Regoli, Ilaria Giuseppina Penco, and Andrea Claudio Cosentini. A clarification of the nuances in the fairness metrics landscape. *Scientific Reports*, 12(1):4209, 2022.
- Junyi Chai and Xiaoqian Wang. Self-supervised fair representation learning without demographics. *Advances in Neural Information Processing Systems*, 35:27100–27113, 2022.
- Hongyan Chang and Reza Shokri. On the privacy risks of algorithmic fairness. In *2021 IEEE European Symposium on Security and Privacy (EuroS&P)*, pages 292–303. IEEE, 2021.
- Laetitia Chapel, Rémi Flamary, Haoran Wu, Cédric Févotte, and Gilles Gasso. Unbalanced optimal transport through non-negative penalized linear regression. *Advances in Neural Information Processing Systems*, 34:23270–23282, 2021.
- Silvia Chiappa. Path-specific counterfactual fairness. In *Proceedings of the AAAI conference on artificial intelligence*, volume 33, pages 7801–7808, 2019.
- Lenaic Chizat, Gabriel Peyré, Bernhard Schmitzer, and François-Xavier Vialard. Scaling algorithms for unbalanced optimal transport problems. *Mathematics of Computation*, 87(314):2563–2609, 2018a.
- Lenaic Chizat, Gabriel Peyré, Bernhard Schmitzer, and François-Xavier Vialard. Unbalanced optimal transport: Dynamic and kantorovich formulations. *Journal of Functional Analysis*, 274(11):3090–3123, 2018b.
- Alexandra Chouldechova. Fair prediction with disparate impact: A study of bias in recidivism prediction instruments. *Big data*, 5(2):153–163, 2017.
- Evgenii Chzhen, Christophe Denis, Mohamed Hebiri, Luca Oneto, and Massimiliano Pontil. Fair regression with Wasserstein barycenters. *Advances in Neural Information Processing Systems*, 33:7321–7331, 2020.
- Evgenii Chzhen, Christophe Giraud, and Gilles Stoltz. A unified approach to fair online learning via blackwell approachability. *Advances in Neural Information Processing Systems*, 34:18280–18292, 2021.
- Nicolas Courty, Rémi Flamary, Amaury Habrard, and Alain Rakotomamonjy. Joint distribution optimal transportation for domain adaptation. *Advances in neural information processing systems*, 30, 2017.

- Elliot Creager, David Madras, Jörn-Henrik Jacobsen, Marissa Weis, Kevin Swersky, Toniann Pitassi, and Richard Zemel. Flexibly fair representation learning by disentanglement. In *International conference on machine learning*, pages 1436–1445. PMLR, 2019.
- Rachel Cummings, Varun Gupta, Dhamma Kimpara, and Jamie Morgenstern. On the compatibility of privacy and fairness. In *Adjunct publication of the 27th conference on user modeling, adaptation and personalization*, pages 309–315, 2019.
- Céline Dard, Hélène Fricker-Hidalgo, Marie-Pierre Brenier-Pinchart, and Hervé Pelloux. Relevance of and new developments in serology for toxoplasmosis. *Trends in parasitology*, 32(6):492–506, 2016.
- Cynthia Dwork, Moritz Hardt, Toniann Pitassi, Omer Reingold, and Richard Zemel. Fairness through awareness. In *Proceedings of the 3rd innovations in theoretical computer science conference*, pages 214–226, 2012.
- Ivar Ekeland and Roger Temam. *Convex analysis and variational problems*. SIAM, 1999.
- Hadi Elzayn, Emily Black, Patrick Vossler, Nathanael Jo, Jacob Goldin, and Daniel E. Ho. Optimal transport in some fairness scenarios, 2023.
- Alessandro Fabris, Andrea Esuli, Alejandro Moreo, and Fabrizio Sebastiani. Measuring fairness under unawareness of sensitive attributes: A quantification-based approach. *Journal of Artificial Intelligence Research*, 76:1117–1180, 2023.
- Michael Feldman, Sorelle A Friedler, John Moeller, Carlos Scheidegger, and Suresh Venkatasubramanian. Certifying and removing disparate impact. In *proceedings of the 21th ACM SIGKDD international conference on knowledge discovery and data mining*, pages 259–268, 2015.
- Alessio Figalli. The optimal partial transport problem. *Archive for rational mechanics and analysis*, 195(2):533–560, 2010.
- Gunnar Friede, Timo Busch, and Alexander Bassen. ESG and financial performance: aggregated evidence from more than 2000 empirical studies. *Journal of Sustainable Finance & Investment*, 5(4):210–233, 2015. doi: 10.1080/20430795.2015.1118917.
- Wilfrid Gangbo and Andrzej Świech. Optimal maps for the multidimensional monge-kantorovich problem. *Communications on Pure and Applied Mathematics: A Journal Issued by the Courant Institute of Mathematical Sciences*, 51(1):23–45, 1998.
- Paula Gordaliza, Eustasio Del Barrio, Gamboa Fabrice, and Jean-Michel Loubes. Obtaining fairness using optimal transport theory. In *International conference on machine learning*, pages 2357–2365. PMLR, 2019.
- Thibaut Le Gouic, Jean-Michel Loubes, and Philippe Rigollet. Projection to fairness in statistical learning. *arXiv preprint arXiv:2005.11720*, 2020.
- Arthur Gretton, Karsten M Borgwardt, Malte J Rasch, Bernhard Schölkopf, and Alexander Smola. A kernel two-sample test. *The Journal of Machine Learning Research*, 13(1):723–773, 2012.

- Nina Grgić-Hlača, Muhammad Bilal Zafar, Krishna P Gummadi, and Adrian Weller. Beyond distributive fairness in algorithmic decision making: Feature selection for procedurally fair learning. In *Proceedings of the AAAI Conference on Artificial Intelligence*, volume 32, 2018.
- Moritz Hardt, Eric Price, and Nati Srebro. Equality of opportunity in supervised learning. In *Advances in neural information processing systems*, pages 3315–3323, 2016.
- Shahin Jabbari, Matthew Joseph, Michael Kearns, Jamie Morgenstern, and Aaron Roth. Fairness in reinforcement learning. In *International conference on machine learning*, pages 1617–1626. PMLR, 2017.
- Heinrich Jiang and Ofir Nachum. Identifying and correcting label bias in machine learning. In *International Conference on Artificial Intelligence and Statistics*, pages 702–712. PMLR, 2020.
- Ray Jiang, Aldo Pacchiano, Tom Stepleton, Heinrich Jiang, and Silvia Chiappa. Wasserstein fair classification. In *Uncertainty in artificial intelligence*, pages 862–872. PMLR, 2020.
- Fanny Jourdan, Titon Tshiongo Kaninku, Nicholas Asher, Jean-Michel Loubes, and Laurent Risser. How optimal transport can tackle gender biases in multi-class neural network classifiers for job recommendations. *Algorithms*, 16(3):174, 2023.
- Joon Sik Kim, Jiahao Chen, and Ameet Talwalkar. Fact: A diagnostic for group fairness trade-offs. In *International Conference on Machine Learning*, pages 5264–5274. PMLR, 2020.
- Jonathan Korman and Robert McCann. Optimal transportation with capacity constraints. *Transactions of the American Mathematical Society*, 367(3):1501–1521, 2015.
- Jonathan Korman and Robert J McCann. Insights into capacity-constrained optimal transport. *Proceedings of the National Academy of Sciences*, 110(25):10064–10067, 2013.
- Matt J Kusner, Joshua Loftus, Chris Russell, and Ricardo Silva. Counterfactual fairness. In *Advances in Neural Information Processing Systems*, pages 4066–4076, 2017.
- Khang Le, Huy Nguyen, Khai Nguyen, Tung Pham, and Nhat Ho. On multimarginal partial optimal transport: Equivalent forms and computational complexity. In *International Conference on Artificial Intelligence and Statistics*, pages 4397–4413. PMLR, 2022.
- David Liu, Virginie Do, Nicolas Usunier, and Maximilian Nickel. Group fairness without demographics using social networks. In *2023 ACM Conference on Fairness, Accountability, and Transparency*. ACM, jun 2023. doi: 10.1145/3593013.3594091. URL <https://doi.org/10.1145/3593013.3594091>.
- Suyun Liu and Luis Nunes Vicente. Accuracy and fairness trade-offs in machine learning: A stochastic multi-objective approach. *Computational Management Science*, 19(3):513–537, 2022.

- Pranay K Lohia, Karthikeyan Natesan Ramamurthy, Manish Bhide, Diptikalyan Saha, Kush R Varshney, and Ruchir Puri. Bias mitigation post-processing for individual and group fairness. In *Icassp 2019-2019 ieee international conference on acoustics, speech and signal processing (icassp)*, pages 2847–2851. IEEE, 2019.
- Debmalya Mandal, Samuel Deng, Suman Jana, Jeannette Wing, and Daniel J Hsu. Ensuring fairness beyond the training data. *Advances in neural information processing systems*, 33:18445–18456, 2020.
- Ninareh Mehrabi, Fred Morstatter, Nripsuta Saxena, Kristina Lerman, and Aram Galstyan. A survey on bias and fairness in machine learning. *ACM computing surveys (CSUR)*, 54(6):1–35, 2021.
- Vishwali Mhasawade, Yuan Zhao, and Rumi Chunara. Machine learning and algorithmic fairness in public and population health. *Nature Machine Intelligence*, 3(8):659–666, 2021.
- Eduardo Fernandes Montesuma, Fred Ngole Mboula, and Antoine Souloumiac. Recent advances in optimal transport for machine learning. *arXiv preprint arXiv:2306.16156*, 2023.
- Deborah Morgan. Anticipatory regulatory instruments for ai systems: A comparative study of regulatory sandbox schemes. In *Proceedings of the 2023 AAAI/ACM Conference on AI, Ethics, and Society*, pages 980–981, 2023.
- Razieh Nabi, Daniel Malinsky, and Ilya Shpitser. Learning optimal fair policies. In *International Conference on Machine Learning*, pages 4674–4682. PMLR, 2019.
- Razieh Nabi, Daniel Malinsky, and Ilya Shpitser. Optimal training of fair predictive models. In *Conference on Causal Learning and Reasoning*, pages 594–617. PMLR, 2022.
- Harikrishna Narasimhan, Andrew Cotter, Maya Gupta, and Serena Wang. Pairwise fairness for ranking and regression. In *Proceedings of the AAAI Conference on Artificial Intelligence*, volume 34, pages 5248–5255, 2020.
- J Saketha Nath and Pratik Jawanpuria. Statistical optimal transport posed as learning kernel mean embedding. Technical report, Technical report, 2020.
- Sibeth Ndiaye. Nous payons aujourd’hui l’effacement de l’universalisme républicain. *Le Monde*, June 13th, 2020. URL https://www.lemonde.fr/idees/article/2020/06/13/sibeth-ndiaye-nous-payons-aujourd-hui-l-effacement-de-l-universalisme-republicain_6042708_3232.html.
- Ion Necoara and Olivier Fercoq. Linear convergence of random dual coordinate descent on nonpolyhedral convex problems. *Mathematics of Operations Research*, 47(4):2641–2666, 2022.
- Khai Nguyen, Dang Nguyen, The-Anh Vu-Le, Tung Pham, and Nhat Ho. Improving mini-batch optimal transport via partial transportation. In Kamalika Chaudhuri, Stefanie Jegelka, Le Song, Csaba Szepesvari, Gang Niu, and Sivan Sabato, editors, *Proceedings*

- of the 39th International Conference on Machine Learning, volume 162 of *Proceedings of Machine Learning Research*, pages 16656–16690. PMLR, 17–23 Jul 2022. URL <https://proceedings.mlr.press/v162/nguyen22e.html>.
- Hamed Nilforoshan, Johann D Gaebler, Ravi Shroff, and Sharad Goel. Causal conceptions of fairness and their consequences. In *International Conference on Machine Learning*, pages 16848–16887. PMLR, 2022.
- Luca Oneto and Silvia Chiappa. Fairness in machine learning. In *Recent trends in learning from data: Tutorials from the inns big data and deep learning conference (innsbddl2019)*, pages 155–196. Springer, 2020.
- Luca Oneto, Michele Doninini, Amon Elders, and Massimiliano Pontil. Taking advantage of multitask learning for fair classification. In *Proceedings of the 2019 AAAI/ACM Conference on AI, Ethics, and Society*, pages 227–237, 2019.
- Osonde A Osoba and William Welser IV. *An intelligence in our image: The risks of bias and errors in artificial intelligence*. Rand Corporation, 2017.
- Dana Pessach and Erez Shmueli. A review on fairness in machine learning. *ACM Computing Surveys (CSUR)*, 55(3):1–44, 2022.
- Felix Petersen, Debarghya Mukherjee, Yuekai Sun, and Mikhail Yurochkin. Post-processing for individual fairness. *Advances in Neural Information Processing Systems*, 34:25944–25955, 2021.
- Gabriel Peyré. Entropic approximation of Wasserstein gradient flows. *SIAM Journal on Imaging Sciences*, 8(4):2323–2351, 2015.
- Gabriel Peyré, Marco Cuturi, et al. Computational optimal transport. *Foundations and Trends® in Machine Learning*, 11(5-6):355–607, 2019.
- Khiem Pham, Khang Le, Nhat Ho, Tung Pham, and Hung Bui. On unbalanced optimal transport: An analysis of sinkhorn algorithm. In *International Conference on Machine Learning*, pages 7673–7682. PMLR, 2020.
- Drago Plecko and Elias Bareinboim. Causal fairness analysis. *arXiv preprint arXiv:2207.11385*, 2022.
- Drago Plecko and Elias Bareinboim. Causal fairness for outcome control. *arXiv preprint arXiv:2306.05066*, 2023.
- Novi Quadrianto and Viktoriia Sharmanska. Recycling privileged learning and distribution matching for fairness. *Advances in neural information processing systems*, 30, 2017.
- Anthony Quinn, Robert Shorten, Martin Corless, Sarah Boufelja, and Quan Zhou. Optimal transport in some fairness scenarios, 2023. URL <https://drive.google.com/file/d/1BVDDSSuDuI8iwIYju0FijwRb1D51FKAT/view?usp=sharing>. presented at the plenary meeting of the AutoFair project in Athens on Wednesday, 10th May 2023. Available on-line.

- Laurent Risser, Alberto Gonzalez Sanz, Quentin Vincenot, and Jean-Michel Loubes. Tackling algorithmic bias in neural-network classifiers using Wasserstein-2 regularization. *Journal of Mathematical Imaging and Vision*, 64(6):672–689, 2022.
- Vivien Seguy and Marco Cuturi. Principal geodesic analysis for probability measures under the optimal transport metric. *Advances in Neural Information Processing Systems*, 28, 2015.
- Nian Si, Karthyek Murthy, Jose Blanchet, and Viet Anh Nguyen. Testing group fairness via optimal transport projections. In *International Conference on Machine Learning*, pages 9649–9659. PMLR, 2021.
- Chiappa Silvia, Jiang Ray, Stepleton Tom, Pacchiano Aldo, Jiang Heinrich, and Aslanides John. A general approach to fairness with optimal transport. In *Proceedings of the AAAI Conference on Artificial Intelligence*, volume 34, pages 3633–3640, 2020.
- Richard Sinkhorn and Paul Knopp. Concerning nonnegative matrices and doubly stochastic matrices. *Pacific Journal of Mathematics*, 21(2):343–348, 1967.
- Nimit Sohoni, Jared Dunnmon, Geoffrey Angus, Albert Gu, and Christopher Ré. No subclass left behind: Fine-grained robustness in coarse-grained classification problems. In H. Larochelle, M. Ranzato, R. Hadsell, M.F. Balcan, and H. Lin, editors, *Advances in Neural Information Processing Systems*, volume 33, pages 19339–19352. Curran Associates, Inc., 2020. URL https://proceedings.neurips.cc/paper_files/paper/2020/file/e0688d13958a19e087e123148555e4b4-Paper.pdf.
- Max Sommerfeld, Jörn Schrieber, Yoav Zemel, and Axel Munk. Optimal transport: Fast probabilistic approximation with exact solvers. *J. Mach. Learn. Res.*, 20(105):1–23, 2019.
- Rosanna Turrisi, Rémi Flamary, Alain Rakotomamonjy, and Massimiliano Pontil. Multi-source domain adaptation via weighted joint distributions optimal transport. In James Cussens and Kun Zhang, editors, *Proceedings of the Thirty-Eighth Conference on Uncertainty in Artificial Intelligence*, volume 180 of *Proceedings of Machine Learning Research*, pages 1970–1980. PMLR, 01–05 Aug 2022. URL <https://proceedings.mlr.press/v180/turrisi22a.html>.
- Cédric Villani. *Topics in optimal transportation*, volume 58. American Mathematical Soc., 2021.
- Serena Wang, Wenshuo Guo, Harikrishna Narasimhan, Andrew Cotter, Maya Gupta, and Michael Jordan. Robust optimization for fairness with noisy protected groups. *Advances in neural information processing systems*, 33:5190–5203, 2020.
- Moyi Yang, Junjie Sheng, Wenyan Liu, Bo Jin, Xiaoling Wang, and Xiangfeng Wang. Obtaining dyadic fairness by optimal transport. In *2022 IEEE International Conference on Big Data (Big Data)*, pages 4726–4732. IEEE, 2022.
- Muhammad Bilal Zafar, Isabel Valera, Manuel Gomez Rodriguez, and Krishna P Gummadi. Fairness beyond disparate treatment & disparate impact: Learning classification without

- disparate mistreatment. In *Proceedings of the 26th international conference on world wide web*, pages 1171–1180, 2017a.
- Muhammad Bilal Zafar, Isabel Valera, Manuel Gomez Rogriguez, and Krishna P Gummadi. Fairness constraints: Mechanisms for fair classification. In *Artificial intelligence and statistics*, pages 962–970. PMLR, 2017b.
- Muhammad Bilal Zafar, Isabel Valera, Manuel Gomez-Rodriguez, and Krishna P Gummadi. Fairness constraints: A flexible approach for fair classification. *The Journal of Machine Learning Research*, 20(1):2737–2778, 2019.
- Rich Zemel, Yu Wu, Kevin Swersky, Toni Pitassi, and Cynthia Dwork. Learning fair representations. In *International conference on machine learning*, pages 325–333. PMLR, 2013.
- Xianli Zeng, Edgar Dobriban, and Guang Cheng. Fair bayes-optimal classifiers under predictive parity. *Advances in Neural Information Processing Systems*, 35:27692–27705, 2022.
- Han Zhao and Geoffrey J. Gordon. Inherent tradeoffs in learning fair representations. *J. Mach. Learn. Res.*, 23(1), Jan 2022. ISSN 1532-4435.